Dear Sarah Shannon and co-authors

Thank you for re-submitting this manuscript to TC. I appreciate all the work you have put into the revision in order to address the reviewer comments, which really improved the manuscript.

In general, I agree that this is an important contribution to the literature as it reports a novel approach to glacier modelling inside a land surface scheme. I agree with the reviewers that this is more a report about the current progress in this field which should also identify possibilities for improvement.

Please, address carefully the second round of reviewer comments and improve the manuscript accordingly. I fully agree with the reviewer comments and will check if these have been addressed thoroughly prior to any final publication. My own concerns are about the strong model biases and negative NS coefficients in winter and summer: How reliable are the future projections in light of these biases? What are the major improvements that you recommend for future studies?

I am very much looking forward to a detailed point-by-point reply to the reviewer comments and an improved version of the manuscript.

Kind regards

Christian Beer

Dear Christian Beer,

Thank you for your feedback on the manuscript. Please find the responses to your comments and the reviewers comments below.

In response to your comments:

My own concerns are about the strong model biases and negative NS coefficients in winter and summer:

1. **How reliable are the future projections in light of these biases?**

   We are aware that the present-day seasonal mass balance contains a negative bias suggesting that melting is overestimated in the summer and accumulation is underestimated in the winter. The bias may result in an overestimate in future volume loss, although this is uncertain given other factors may have a larger effect in the future, for example uncertainty in the climate forcing.

   The bias is caused by an underestimate in snowfall due to the simple approach to correcting coarse scale gridded precipitation for orographic effects and lapse rate. This problem is not unique to our approach but affects many attempts to use global climate model information to make projections of glacier mass balance. A more nuanced approach could be to use a more detailed regional climate model data that explicitly represent orographic effects. Alternative approaches effectively add a scalar on precipitation to capture orographic enhancement and assume this to be constant under a future climate then as a second step lapse the precipitation across elevation bands. Standing alone these projections may contain larger uncertainties than other global glaciers model, due to bias in the calibration, the coarse nature of JULES and missing processes. The model could however, contribute to the aim of generating reliable future projections, by contributing an alternative type of global glacier model to a glacier model intercomparison exercise.

To ensure we make the point that the bias might cause an overestimate in the volume loss projection we add the following to the top of the discussion

"Our calibrated seasonal mass balance contains a negative bias (accumulation is underestimated, and melting is overestimated) which suggests that the volume loss projections might be overestimated"

2. **What are the major improvements that you recommend for future studies?**
   Firstly, we think calibration approach could be improved. This is certainly the most challenging part of this work. Future work would test if the negative bias in the seasonal mas balance could be reduced or eliminated by scaling the gridbox mean precipitation prior to applying the lapse rate correction. We would also consider extrapolating the precipitation lapse rates to other regions using an empirical relationship which categorises the climate, similar to the work of Radic et al 2014., Also, we would use observations from satellite gravimetry and altimetry, such as that described by Gardner et al (2013) to get a quantitative estimate of the model performance at the regional scales (included in the discussion section P17 Line 12).

   Secondly, we would add a volume-area scaling scheme to remove the limitation of fixed glaciated area (included in the discussion section P17 line 25). We would consider evaluating the scheme over the Alps, because the region is data rich in comparison to other locations and a comparison could be made to the glacier scheme in the REMO regional climate model (Kotlarski et al. 2010).

I have read the paper a second time after the author's revision. The authors invested a lot of energy in the revision, which is recommendable. Some of my comments have been addressed, other have been ignored or implemented differently. Some model results are still dubious to me (mostly: the surprising seasonal mass-balances and the mass fluxes per elevation band). Overall I am still convinced that there is a potential for model improvements, but the current version of the paper discusses the model limitations in an appropriate way. I have a few minor comments listed below and would like to take the opportunity to reply to three topics raised in the interactive discussion. Points raised in the discussion

From the three points below, only point 1 needs concrete action in the manuscript. Points 2 and 3 are here just for the sake of scientific debate.

1. Elevation feedback: From the author's response to Reviewer #1 and myself I found two contradicting statements: To reviewer #1 you wrote: "The negative feedback between terminus elevation and mass balance is missing and the only way for a melting glacier to reach equilibrium with climate is by melting completely." And to my question about whether glaciers can melt on elevation bands you write: "This allows glacier tiles to gain or lose mass at elevation bands". I still have trouble to understand what you actually mean in your answer to reviewer #1 and in the text: if you loose mass at an elevation band you could include an elevation feedback by letting the band's elevation decrease until the bedrock is reached (which you probably won't do because of obvious complications in the code). However, you are able to stop the melt when an elevation band is melted completely. So some negative feedback should already be included in your model, and you might revise the answer to reviewer #1 by saying that the area is left unchanged, which is better than leaving the entire elevation band after it has melted.

You are correct here, there is an elevation feedback, so we will revise the answer to reviewer #1. Part of the reason for the confusion is that the elevation feedback is different to our classical understanding of elevation feedback. For example, in a classical case, if a glacier thickens then the top of the glacier *will experience cooler temperatures. In our case if the snowpack thickens the top of the snowpack doesn't feel that cooler temperature but it experiences the temperature of the elevation band. The elevation feedback in our model is simpler than the classical elevation feedback mechanism.*

Changes to manuscript:

We added the following to the model description section (P4 L13)

"The scheme assumes that the snowpack can grow or shrink at elevation bands depending on the mass balance, but that tile fraction (derived from the glacier area) is static with time. The ability to grow or shrink the snowpack at elevation levels means that the model includes a simple elevation feedback mechanism. If the snowpack shrinks to zero at an elevation band, then the terminus of the glacier moves to the next level above. On the other hand, if the snowpack grows at an elevation band it just continues to grow and there is no process to move the ice from higher elevations to lower elevations. Typically, in an elevation feedback, when a glacier grows the surface of the glacier will experience a cooler temperature, however in this case, the snowpack surface experiences the temperature of the elevation band."

We removed the following text P16 L18 and the citation of Marzeion et al (2014) in the reference list.

Another explanation why we predict more volume loss than Radic et al. (2014) and Huss and Hock (2015) is because there is no retreat of the glacier terminus represented in the model. The only way for glaciers to reach equilibrium with climate is by melting completely. A study by Marzeion et al. (2014) showed that models predict more mass loss when the terminus elevation is fixed than when it is allowed to vary. This is because when the terminus is allowed to retreat, there will be less area available to melt. Marzeion et al (2014) found that neglecting terminus elevation changes resulted in an extra few tens of mm SLE depending on RCP scenario. Lastly, some of the differences between our study and other published projections could be due models using different initial ice volumes and glaciated areas.

2. Regional parameter sets. To my comment about regional calibration, you write: "It is not clear why a single global parameter set would be more robust than regional parameters sets." Let me make an example based on JULES. How would it be if the model parameters for, say, "clay porosity" or "tree leave albedo" would be different between England and Wales? The equations of wind motion or ice melt do not follow arbitrary frontiers. I might be wrong, but this glacier module is probably the first module in JULES to use regional parameter sets. Don't get me wrong: I understand that parameters need to be tuned, especially in a "physically based model" with many parameters. I just say that using parameters based on RGI regions is suboptimal, for several reasons: - it creates unphysical differences between neighboring regions (such as 13, 14, 15 in High Asia) - it hides model deficiencies (or errors in forcing data) by tuning the model on a smaller set of observations (sometimes only one or two glaciers per region) - in a global model like JULES, it will hinder the acceptance by the wider community and the module will have more difficulties to enter the main codebase

We agree with your point that this approach will result in arbitrary thresholds between adjacent regions. As you know the motivation for using regional parameter sets is because different regions have different process (for example debris cover is more prevalent in Himalayan glaciers than Alpine glaciers). If the model included more processes, for instances avalanching, blowing snow etc..) then there would be no need to have regional parameters.

There are examples in JULES where regional parameter sets are used. For example

- *Later configurations which use spatially varying albedo properties based on satellite ancillaries*
- *Different fresh snow density in the UK configuration compared to the global*

In terms of JULES, there are no barriers for the inclusion of the module into the code base, however, the way in which the glacier scheme is used in specific model configurations is likely to require more work.

2. Energy balance

In the revised version you added analyses of mass fluxes (which can be done by more simple models like degree-day models as well), but not of energy fluxes. I believe this is a missed opportunity.

Apologies, I miss-interpreted your request as asking for mass fluxes per elevation, hence the extra analysis of this. We have added some extra material on the future global energy fluxes. Since the manuscript is already quiet long, we have kept the extra material brief. An analysis of how the fluxes vary regionally and with height would be interesting for a follow up paper.

Changes to manuscript:

We added an extra figure (Fig 11) showing the ensemble mean energy balance components for all glaciated regions averaged over all elevation levels.

We also added the following text to section 4.2 Regional glacier volume projections 2011-2097

*"To investigate which parts of the energy balance are driving the future melt rates, we show the energy balance components averaged over all regions and all elevation levels in **Error! Reference source not found.**. Future melting is caused by a positive net radiation of approximately 30 Wm^{-2} that is sustained throughout the century. This is comprised of 18 Wm^{-2} net shortwave, 3 Wm^{-2} net longwave, 5 Wm^{-2} latent heat flux and 4 Wm^{-2} sensible heat flux. The largest component of the radiation for melting comes from the net shortwave radiation. The upward shortwave radiation comprises of direct and diffuse components in the visible and near infrared wavelengths. The visible albedo deceases because melting causes the ice surface to darken. In contrast, the near infrared albedo increases because the ice is heating up emitting radiation in the infrared part of the spectrum. The downward and upward longwave radiation are increasing in future however, the net longwave radiation contribution to the melting is small. The downward longwave radiation increases because of the T^4 relationship with air temperature, whereas the upward longwave radiation increases because the glacier surface is warming. The latent heat flux from refreezing of melt water and the sensible heat from surface warming are also small components of the net radiation balance."*

Detailed comments P6 L26-27: remove "this is because..."

Deleted "this is because..."

P9 L6: add Marzeion et al., 2012 to the references list.

Reference added

P10 L23: please add reasons for the negative bias. In linear a model with enough degrees of freedom, minimizing RMSD will always minimize the bias too. So the first thing that comes to mind is stat systematic problems in the model and/or the forcing data are preventing this bias minimization

(confirmed by the supplementary analyses). In short: there seems to be a structural problem in either the model or the forcing data.

We agree that minimising the RMSE should also minimise the bias unless there is some structural problem preventing this. Perhaps increasing the upper bound for the tuneable precipitation gradient might help this, since we found that minimising the bias resulted in a preference for higher precipitation gradients. Our upper bound is 25%/100m but the work of Rye (2012) found optimum values as high as 45% to 51%/100m for glaciers in Svalbard. If this work were to be repeated, we would recommend improving the way the precipitation lapse rate is implemented in the model.

The explanation for the negative biases is included in Section 3.2 so instead of repeating the material we add

Changes to manuscript:

" The negative bias is also seen in the summer and winter mass balance and discussed in Section 3.2"

We also updated section 3.2 to answer a comment by Reviewer #1 as to why the model predicts some negative winter mass balance and some positive summer mass balance. Please see our reply to this below.

P10 L29: "Our mass balance model does include sublimation". I am curious: since you have a latent heat flux, why don't you simply convert it to a mass loss? This is the typical way to compute sublimation in glacier energy and mass balance models.

*Perhaps there is a mis-communication here. We write that our model 'does include' sublimation. Sublimation is calculated by the surface exchange module in JULES. To avoid confusion, we change this to 'our model **includes** sublimation'*

Figure 4: you might consider add Maladeta to Figure 3 and spare a figure.

Changes to manuscript: We deleted Figure 4 and included it in Figure 3 (see black circles)

Table 6: consider making a bar-plot out of it for more readability

We did not make a bar-chart of Table 6 because we included an extra figure in the supplementary material to show the future cumulated mass balances at elevation levels for each RGI6 region (Fig. S8). The volume change per height in Fig S8 is more meaningful than the percentage changes listed in columns 5-7 of Table 6. For example, in Alaska for elevation ranges 4250m-8000m there is 408 % volume increase, but this does not translate to a large volume increase because there is very little glaciated area at these elevation bands.

Changes to manuscript: None

P13 L30: here you talk about sublimation. This contradicts your statement above.

*Please see our reply above confirming that sublimation **is** included in the model.*

Fig. 12: to make the figure more readable you could remove the x and y axis labels for the interior plots, since they are the same for each plot.

Changes to manuscript: The x and y axis labels for the interior plots are removed.

Figure 13 and corresponding analysis in the text: I have trouble to understand why the upper elevations see a reduction in melt while the lower parts do not? The provided explanation

("reduction in mass loss as glaciers disappear towards the end of the century" holds even more true for lower elevations.

Or is this due to regional differences, the high latitude arctic having more mass below 2000 m a.s.l? This needs more explanation in the text.

Yes, you are correct. The reason there is no reduction in melt rates below 2000m is because there are still large amounts of ice available to melt at high latitudes.

Changes to manuscript: We added the text below and Figure S8 to the supplementary material to show the future cumulated mass balances as a function of height.

"Figure 12 shows how the global annual mass balance components vary with time for low, medium and high elevations ranges. There is a reduction in accumulation and refreezing at all elevation ranges towards the end of the century. Melt rates decreases at medium and high elevation ranges because glaciers mass is lost at these altitudes, therefore less ice is available to melt (see Fig. S8 for the future cumulated mass balances as a function of height). Melt rates are constant at the low elevation ranges because there remains substantial quantities of ice available to melt at the end of the century in Greenland, Arctic Canada North and South, Svalbard, Russian Arctic.

P16-L16: about elevation feedback - see main comment above.

We removed this text. Please see our reply to this above.

P18 L20: "Changes in solar radiation can be an important driver of melting.": It is a bit sad that you didn't take my advice about analysing the energy fluxes...

Please see our reply to this above and the following changes to the manuscript:

We added the following to the discussion: "In this paper, we present a brief analysis of the future global energy balance fluxes, but how the fluxes vary for individual regions and elevation levels could be investigated further. "

I would like to thank the authors for the thoughtful, and in most cases, satisfactory responses to my review comments. In particular, I want to compliment them on performing a substantial amount of additional runs, including alternative optimization approaches. Those additional analyses and results make the manuscript a lot stronger and help to better understand and evaluate the results. I hope the authors would agree that there are still a number of issues with the model that will eventually need to be addressed, but given that this is a very new approach to modeling glaciers on the global scale (and one has to start somewhere), I think the comprehensive presentation of the validation results, and the discussion of the (in some cases problematic) model behaviour warrants a publication in The Cryosphere.

There are just two minor comments that should be addressed prior to publication, and I have one suggestion that the author may consider for the further development of the model:

- My comment on P10 L1f does not seem to have been addressed.

Your original comment was "The tropical glaciers are really small; there are probably numerous more likely explanations for a warm bias than glaciers lacking in the model.

Change to manuscript: We removed the text "It is possible that the ECMWF model does not include glacier ice in tropical regions. The absence of ice to cool the lower atmosphere would make the grid box mean temperature too warm".

- With my comment on Fig 6 and 7 (negative winter MBs and positive summer MBs) I did not want to imply that from a warm bias in winter follows a cold bias in summer (sorry for the confusion), but I wanted to suggest that it should be discussed why there are so many negative winter MB values (as well as quite a few positive summer MB values). Typically, winter and summer values are well separated by the zero line (see, e.g., Fig. 3 in Radic et al., 2014).

The negative mass balance in winter and positive mass balance in summer at some sites is caused by the simple treatment of the precipitation lapse rate in the model.

We added the following text by way of explanation to the model validation section 3.2. An extra two figures have been added to the Supplementary material to show the mass balance components for two glaciers, one which negative winter mass balance and another which has positive summer mass balance (Fig. S9 and S10).

Changes to manuscript:

The reason for the negative bias is because the model underestimates the precipitation and therefore the accumulation part of the mass balance is underestimated. This is because our approach to correcting the coarse scale gridded precipitation for orographic effects is simple. We use a single precipitation gradient for each RGI6 region and do not apply a bias correction. A bias correction is often recommended because precipitation is underestimated in coarse resolution datasets. Gauging observations are sparse in high mountains regions and snowfall observations can be susceptible to undercatch by 20–50% (Rasmussen et al. 2012). Our precipitation rates are generally too low because we do not bias correct the precipitation.

Other studies use a bias correction that varies regionally (Radic and Hock 2011, Radic et al. 2014, Bliss et al. 2014). In those studies, the precipitation at the top of the glacier was estimated using a bias correction factor k_p. The decrease in precipitation from the top of the glacier to the snout was calculated using a precipitation gradient. To account for the fact that the mass balance of maritime and continental glaciers respond differently to precipitation changes k_p was related to a continentality index. Our motivation for using a single precipitation gradient for each RGI6 region, and no bias correction was to test the simplest approach first, however the resulting biases suggest that this approach could be improved.

The impact of underestimating the precipitation is that we simulate negative mass balance in winter at some observational sites (Fig 5(A) and Fig 4.). To demonstrate this, we compare the mass balance components for two glaciers; the Leviy Aktru in the Russian Altai Mountains which has negative mass balance in the winter and Kozelskiy glacier in North Eastern Russia which has no negative mass balance in the winter (See Fig. S9). Both glaciers are in the North Asia RGI6 region, so have the same tuned parameters for mass balance. The simulated winter accumulation rates are much lower at Leviy Aktru glacier than Kozelskiy glacier leading to negative mass balance at the lowest 3 model levels below 2750m.

The simplistic treatment of the precipitation lapse rate also leads to instances where the model simulates positive mass balance in the summer at some locations (Fig 6 (A) and Fig 4.). We show the summer mass balance components for the same two glaciers in Fig S10. Positive mass balance is simulated at Kozelskiy glacier because accumulation exceeds the melting. This suggests that the precipitation gradient (19% per 100m for North Asia) is overly steep in the summer at this location.

Finally, just an idea to consider, concerning the issue of water mass conservation being affected by the precipitation lapse rate (page 6, line 3): The authors correctly point out that a precipitation lapse rate is standard in glacier modeling (effectively increasing precipitation to the glacier surface compared to the data set used as boundary condition), and it makes sense because wind-blown snow and avalanching are important components of the mass balance of many glaciers – i.e., there is in fact horizontal redistribution of precipitation to the glaciers. One way to conserve mass would be to reduce the precipitation onto the non-glaciated area of the grid cell, which would be conceptually consistent with horizontal mass movement within the grid box.

Thank you for this suggestion. We added this to the discussion

Changes to manuscript:

Added this text P17 L24

"Another limitation of the model, which may be problematic for same applications, is that the gridbox mean precipitation is not conserved when precipitation is adjusted for elevation. This correction was necessary to get enough accumulation in the mass balance at high elevations. One way to conserve water mass would be to reduce the precipitation onto the non-glaciated area of the grid cell. This would represent horizontal mass movement within the grid box from wind-blown snow and avalanching."

Kotlarski, S., D. Jacob, R. Podzun & F. Paul (2010) Representing glaciers in a regional climate model. *Climate Dynamics,* 34**,** 27-46.

Marzeion, B., A. H. Jarosch & J. M. Gregory (2014) Feedbacks and mechanisms affecting the global sensitivity of glaciers to climate change. *Cryosphere,* 8**,** 59-71.

Radic, V., A. Bliss, A. C. Beedlow, R. Hock, E. Miles & J. G. Cogley (2014) Regional and global projections of twenty-first century glacier mass changes in response to climate scenarios from global climate models. *Climate Dynamics,* 42**,** 37-58.

Rye, C. J., I. C. Willis, N. S. Arnold & J. Kohler (2012) On the need for automated multiobjective optimization and uncertainty estimation of glacier mass balance models. *Journal of Geophysical Research-Earth Surface,* 117.

Global glacier volume projections under high-end climate change scenarios

Sarah Shannon[1,2], Robin Smith[3], Andy Wiltshire[4], Tony Payne[2], Matthias Huss[5,6], Richard Betts[1,4], John Caesar[4], Aris Koutroulis[7], Darren Jones[8] and Stephan Harrison[8]

[1]School of Geography, The University of Exeter, The Queen's Drive, Exeter, Devon, EX4 4QJ, UK
[2]Bristol Glaciology Centre, Department of Geographical Science, University Road, University of Bristol, BS8 1SS, UK
[3]NCAS-Climate, Department of Meteorology, University of Reading, Reading, RG6 6BB, UK
[4]Met Office, Fitzroy Road, Exeter, Devon, EX1 3PB, UK
[5]Department of Geosciences, University of Fribourg, Fribourg, Switzerland
[6]Laboratory of Hydraulics, Hydrology and Glaciology, ETH Zurich, Zurich, Switzerland
[7]School of Environmental Engineering, Technical University of Crete, Akrotiri, 73100 Chania, Greece
[8]University of Exeter, Penryn Campus, Treliever Road, Penryn, Cornwall, TR10 9FE, UK

Correspondence to: S. R. Shannon (sarah.shannon@bristol.ac.uk)

Abstract.

The Paris agreement aims to hold global warming to well below 2°C and to pursue efforts to limit it to 1.5°C relative to the pre-industrial period. Recent estimates based on population growth and intended carbon emissions from participant countries, suggest global warming may exceed this ambitious target. Here we present glacier volume projections for the end of this century, under a range of high-end climate change scenarios, defined as exceeding +2 °C global average warming relative to the preindustrial period. Glacier volume is modelled by developing an elevation-dependent mass balance model for the Joint UK Land Environmental Simulator (JULES). To do this, we modify JULES to include glaciated and un-glaciated surfaces that can exist at multiple heights within a single grid-box. Present day mass balance is calibrated by tuning albedo, wind speed, precipitation and temperature lapse rates to obtain the best agreement with observed mass balance profiles. JULES is forced with an ensemble of six Coupled Model Intercomparison Project Phase 5 (CMIP5) models which were downscaled using the high resolution HadGEM3-A atmosphere only global climate model. The CMIP5 models use the RCP8.5 climate change scenario and were selected on the criteria of passing ~~JULES is forced with an ensemble of six Coupled Model Intercomparison Project Phase 5 (CMIP5) models which were downscaled using the high resolution HadGEM3-A atmosphere only global climate model.~~ ~~each~~2°C global average warming during this century. The ensemble mean volume loss at the end of the century plus/minus one standard deviation is, -64±5% for all glaciers excluding those on the peripheral of the Antarctic ice sheet. The uncertainty in the multi-model mean is rather small and caused by the sensitivity of HadGEM3-A to the boundary conditions supplied by the CMIP5 models. The regions which lose more than 75% of their initial volume by the end of the century are; Alaska, Western Canada and US, Iceland, Scandinavia, Russian Arctic, Central Europe, Caucasus, High Mountain Asia, Low Latitudes, Southern Andes and New Zealand. The ensemble mean ice loss expressed in sea-level equivalent contribution is 215.2 ± 21.3 mm. The largest contributors to sea-level rise are Alaska (44.6 ± 1.1mm), Arctic Canada North and South (34.9

± 3.0mm), Russian Arctic (33.3 ± 4.8mm), Greenland (20.1±4.4), High Mountain Asia (combined Central Asia, South Asia East and West), (18.0 ± 0.8mm), Southern Andes (14.4 ± 0.1mm) and Svalbard (17.0 ± 4.6mm). Including parametric uncertainty in the calibrated mass balance parameters, gives an upper bound global volume loss of 281.1~~247.3~~ mm, sea-level equivalent by the end of the century. Such large ice losses will have inevitable consequences for sea-level rise and for water supply in glacier-fed river systems.

1 Introduction

Glaciers act as natural reservoirs by storing water in the winter and releasing it during dry periods.~~ when demand for water is high.~~ This is particularly vital for seasonal water supply ~~for~~in large river systems in South Asia (Immerzeel, 2013;Lutz et al., 2014;Huss and Hock, 2018) and Central Asia (Sorg et al., 2012) where glacier melting contributes to streamflow and supplies fresh water to millions of people downstream. Glaciers are also major contributors to sea~~-~~level rise, despite their mass being much smaller than the Greenland and Antarctic ice sheets (Kaser et al., 2006;Meier et al., 2007;Gardner et al., 2013). Since glaciers are expected to lose mass into the twenty first century (Radić et al., 2014;Giesen and Oerlemans, 2013;Slangen et al., 2014;Huss and Hock, 2015), there is an urgent need to understand how this will affect seasonal water supply and food security. To study this requires a fully integrated impacts model which includes the linkages and interactions between glacier mass balance, river runoff, irrigation and crop production.

The Joint UK Land Environment Simulator (JULES) (Best et al., 2011) is an appropriate choice for this task because it models these processes, but is currently missing a representation of glacier ice. JULES is the land surface component of the Met Office Global Climate Model (GCM), which is used for operational weather forecasting and climate modelling studies. JULES was originally developed to model vegetation dynamics, snow and soil hydrological processes within the GCM but now has a crop model to simulate crop yield for wheat, soybean, maize and rice (Osborne, 2014), an irrigation demand scheme to extract water from ground and river stores and two river routing schemes; Total Runoff Integrating Pathways (Oki, 1999)(TRIP) and the RFM kinematic wave model (Bell et al., 2007). The first objective of this study is to add a glacier ice scheme to JULES to contribute to the larger goal of developing of a fully integrated impacts model.

The second objective is to make projections of glacier volume changes under high-end climate change scenarios, defined as exceeding 2 °C global average warming relative to the preindustrial period (2017). The Paris agreement aims to hold global warming to well below 2ºC and to pursue efforts to limit it to 1.5ºC relative to the pre-industrial period (UNFCCC 2015), however, there is some evidence that this target may be exceeded. Revised estimates of population growth suggests there is only a 5% chance of staying below 2 °C and that the likely range of temperature increase will be 2.0–4.9 °C (Raftery et al., 2017). A global temperature increase of 2.6–3.1 °C has been estimated based on the intended carbon emissions submitted by the participant countries for 2020 (Rogelj et al., 2016). Therefore, in this study we make end of the century glacier volume projections, using a subset of downscaled Coupled Model Intercomparison Project phase 5 (CMIP5) models which pass 2ºC and 4°C global average warming. The CMIP5 models use the Representative Concentration Pathways (RCP) RCP8.5 climate change scenario for high greenhouse gas emissions.

The paper is organised as follows; In Section 2 we describe the glacier ice scheme implemented in JULES and the procedure for initialising the model. Section 3 describes how glacier mass balance is calibrated and validated for the present day. Section 4 presents future glacier volume projections, a comparison with other studies and a discussion on parametric uncertainty in the calibration procedure. Section 5 discusses the results, the model limitations and areas for future development. In Section 6, we summarise our findings with some concluding remarks.

2 Model description

JULES (described in detail by Best et al. (2011)) characterises the land surface in terms of sub-grid scale tiles representing natural vegetation, crops, urban, bare soil, lakes and ice. Each grid box is comprised of fractions of these tiles with the total tile fraction summing to 1. The exception to this, is the ice tile which cannot co-exist with other surface types in a grid box. A grid box is either completely covered in ice or not. All tiles can be assigned ~~an~~ elevation offsets from the grid box mean which is typically set to zero as default.

To simulate the mass balance of mountain glaciers more accurately we extend the tiling scheme to flexibly model the surface exchange in different elevation classes in each JULES gridbox. We have added two new surface types, glaciated and unglaciated elevated tiles to JULES (version 4.7) to describe the areal extent and variation in height of glaciers in a gridbox (Fig. 1). Each of these new types, at each elevation, has its own bedrock sub-surface with a fixed heat capacity. These sub-surfaces are impervious to water, and have no carbon content, so have no interaction with the complex hydrology or vegetation found in the rest of JULES. Because glaciated and unglaciated elevated tiles have their own separate bedrock sub-surface they are not allowed to share a gridbox with any other tiles. For instance, gridboxes cannot contain partial coverage of elevated glacier ice and vegetated tiles.

JULES is modified to enable tile heights to be specified in meters above sea level, as opposed to the default option, which is to specify heights as offsets from the gridbox mean. This makes it easier to input glacier hypsometry into the model and to compare the output to observations for particular elevation bands. To implement this change, the gridbox mean elevation associated with the forcing data, is read in as an additional ancillary file. Downscaling of the climate data, described in Section 2.1, is calculated using the difference between the elevation band (z_{band}) and the gridbox mean elevation (z_{gbm})

$$\Delta z = z_{band} - z_{gbm} \quad \textbf{(1)}$$

For the purposes of this study JULES is set up with a spatial resolution of 0.5-degree and 46 elevation bands ranging from 0 - 9000m in increments of 250m. The horizontal resolution of 0.5-degree is used because it matches the forcing data used to drive the model. The vertical resolution of 250m was used based on computational cost. The vertical and horizontal resolutions of the model can be modified for any setup ~~for another type of model setup~~.

Each elevated glacier tile has a snowpack which ~~JULES has a full energy balance multi-level snowpack scheme which~~ can ~~models~~ gain mass through accumulation and freezing of water and lose mass through sublimation and~~,~~ melting.~~,~~ JULES has a ~~compaction and refreezing in the snowpack. The~~ full energy balance multi-level snowpack scheme which ~~is~~ splits the snowpack into layers each having a thickness, temperature, density, grain size (used to determine albedo), and solid ice and liquid water contents. The initialisation of the snowpack properties and the distribution of the glacier tiles as a function of height is described in section 2.3. Fresh snow accumulates at the surface of the snowpack at a characteristic low density and compacts towards the bottom o~~-~~f the snowpack under the force of gravity. When rain falls on the snowpack, water is percolated through the layers if the pore space is sufficiently large, while any excess water contributes to the surface runoff. Liquid water below the melting temperature can refreeze. A full energy balance model is used to calculate the energy available for melting. ~~Mass may be removed by sublimation at the surface, or by melting which is implied by the energy balance at each depth.~~ If all the mass in a layer is removed within a model timestep then removal takes place in the layer below. The temperature at each snowpack level is calculated by solving a set of tridiagonal equations for heat transfer with the surface boundary temperature set to the air temperature and the bottom boundary temperature set to the sub-surface temperature.

~~Water can percolate through the snowpack if the pore space is sufficiently large and any liquid water below the melting temperature can refreeze.~~ A ~~S~~snowpack~~s~~ may exist on both glaciated and unglaciated elevated tiles if there is accumulation of snow.

The elevation-dependent mass balance ($SMB_{z,t}$) is calculated as the change in the snowpack mass (S) between successive time steps

$$\boldsymbol{SMB_{z,t} = S_{z,t} - S_{z,t-1}} \qquad \textbf{(2)}$$

The scheme assumes that the snowpack can grow or shrink at elevation bands depending on the mass balance, but that tile fraction (derived from the glacier area) is static with time. The ability to grow or shrink the snowpack at elevation levels means that the model includes a simple elevation feedback mechanism. If the snowpack shrinks to zero at an elevation band, then the terminus of the glacier moves to the next level above. On the other hand, if~~when~~ the snowpack grows at an elevation band~~s~~ it just continues to grow and there is no process to move the ice from higher elevations to lower elevations. Typically, in an elevation feedback, when a glacier grows the surface of the glacier will experience a cooler temperature, however in this case, the snowpack surface experiences the temperature of the elevation band.

2.1 Downscaling of climate forcing on elevations

Both glaciated and unglaciated elevated tiles are assigned heights in meters above sea level and the following adjustments are made to the surface climate in gridboxes where glaciers are present.

2.2.1 Air temperature and specific humidity

Temperature is adjusted for elevation using a dry and moist adiabatic lapse rate depending on the dew point temperature. First the elevated temperature follows the dry adiabat

$$\boldsymbol{T_z = T_0 - \gamma_{dry} \Delta z} \tag{3}$$

where T_0 is the surface temperature, γ_{dry} is the dry adiabatic temperature lapse rate (°Cm^{-1}) and Δz is the height difference between tile elevation and the gridbox mean elevation associated with the forcing data.

If the T_z is less than the dew point temperature T_{dew} then the temperature adjustment follows the moist adiabat. A moist adiabatic lapse rate is calculated using the surface specific humidity from the forcing data

$$\boldsymbol{\gamma_{moist} = \frac{\left(\frac{g(1+lc.q_0)}{r.T_v(1-q_0)}\right)}{\left(\frac{C_p+lc.2.q_0.R}{r.T_v2.(1-q_0)}\right)}} \tag{4}$$

q_0 is the surface specific humidity, l_c is the latent heat of fusion of water at 0°C (2.501 x 10^6 J kg^{-1})~~)~~, g is the acceleration due to gravity (9.8 ms^{-2}~~^{1}~~), r is the gas constant for dry air (287.05 kg K^{-1})~~,~~ R is the ratio of molecular weights of water and dry air (0.62198) and T_v (K) is the virtual dew point temperature

$$\boldsymbol{T_v = T_{dew}\left(1 + \left(\frac{1}{R} - 1.0\right).q_0\right)} \tag{5}$$

The height at which the air becomes saturated z is

$$\boldsymbol{z = \frac{T_0 - T_{dew}}{\gamma_{dry}}} \tag{6}$$

The elevated temperature following the moist adiabat is then

$$\boldsymbol{T_z = T_{dew} - (\Delta z - z)\gamma_{moist}} \tag{7}$$

Additionally, when $T_z < T_{dew}$, the specific humidity is adjusted for height. The adjustment is made using the elevated air temperature and surface pressure from the forcing data using a lookup table based on Goff-Gratch formula ~~Goff-Grate formula~~ (Landolt-Bornstein, 1987). The adjusted humidity is then used in the surface exchange calculation. ~~For simplification we only tune the dry adiabatic lapse rate in this study (see Section 3).~~

2.2.2 Longwave radiation

Downward longwave radiation is adjusted by assuming the atmosphere behaves as a black body using Stefan-Boltzmann's law. The radiative air temperature at the surface $T_{rad,0}$ is calculated using the downward longwave radiation provided by the forcing data $LW_{\downarrow z0}$

$$\boldsymbol{T_{rad,0} = \left(\frac{LW_{\downarrow z0}}{\sigma}\right)^{\frac{1}{4}}} \tag{8}$$

Where σ is the Stefan-Boltzmann constant (5.67 x 10^{-8} W m^{-2} K^{-4}). The radiative temperature at height is then adjusted

$$\boldsymbol{T_{rad,z} = T_{rad,0} + T_z - T_0} \tag{9}$$

Formatted: Subscript

Formatted: Not Superscript/ Subscript

Where T_0 is the grid box mean temperature from the forcing data and T_z is the elevated air temperature. This is used to calculate the downward longwave radiation $LW_{\downarrow z}$ at height

$$LW_{\downarrow z} = \sigma T^4_{rad,z} \tag{10}$$

An additional correction is made to ensure that the gridbox mean downward longwave radiation is preserved

$$LW_{\downarrow z} = LW_{\downarrow z} - \sum_{z=1}^{n} LW_{\downarrow z} . frac(z) \frac{|LW_{\downarrow z}|}{\sum_{i=1}^{z} |LW_{\downarrow z}| . frac(z)} \tag{11}$$

where frac is the tile fraction.

2.2.3 Precipitation

To account for orographic precipitation, large scale and convective rainfall and snowfall are adjusted for elevation using an annual mean precipitation gradient (%/100m)

$$P_z = P_0 + P_0\, \gamma_{precip}(z - z_0) \tag{12}$$

where P_0 is the surface precipitation, γ_{precip} is the precipitation gradient and Z_0 is the grid box mean elevation. Rainfall is also converted to snowfall when the elevated air temperature T_z is less the melting temperature (0ºC). The adjusted precipitation fields are input into the snowpack scheme and the hydrology subroutine. When calibrating the present-day mass balance, we needed to lapse rate correct the precipitation to get sufficient accumulation in the mass balance compared to observations. The consequence of this, is that the gridbox mean precipitation is no longer conserved. We tested scaling the precipitation, in a way that conserves the gridbox mean by reducing the precipitation near the surface and increasing it at height, but this did not yield enough precipitation to get a good agreement with the mass balance observations. If the model is being used to simulate river discharge in glaciated catchments, then the precipitation lapse rate could be used as a parameter to calibrate the discharge.

2.2.4 Wind speed

A component of the energy available to melt ice, comes from the sensible heat flux which is related to the temperature difference between the surface and the elevation level and the wind speed.

Glaciers often have katabatic (downslope) winds which enhance the sensible heat flux and increase melting (Oerlemans and Grisogono, 2002). It is important to represent the effects of katabatic winds on the mass balance when trying to model glacier melt, particularly at lower elevations where the katabatic winds speed is highest.

To explicitly model katabatic winds would require knowledge of the gridbox mean slope at elevation bands, so instead a simple scaling of the surface wind speed is used to represent katabatic winds. Over glaciated grid boxes the wind speed is

$$u_z = u_0 \gamma_{wind} \tag{13}$$

where γ_{wind} is a wind speed scale factor and u_0 is the surface wind speed. The simple scaling increases the wind speed relative to the surface forcing data and assumes that the scaling is constant for all heights.

Although our approach is rather crude, we found that scaling the wind speed was necessary to get reasonable values for the sensible heat flux. This is seen when we ~~We~~ compare~~ed~~ the modelled energy balance components to observations from the Pasterze glacier in the Alps (Greuell and Smeets, 2001). The measurements consist of incoming and outgoing short and long wave radiation, albedo, temperature, wind speed and roughness length at five heights between 2205m-3325m meters above sea level on the glacier. Table S6 in the Supplementary Material lists the observed and modelled energy balance components and meteorological data, for experiments with and without wind speed scaling. The comparison shows that JULES underestimates the sensible heat flux by at least one order of magnitude and~~. T~~ the modelled wind speed is four times lower than the observations. When we increase the wind speed to match the observations there is a better agreement with the observed sensible heat flux. ~~This is because t~~The surface exchange coefficient ~~,~~ which is used to calculate the sensible heat flux~~,~~ is a function of the wind speed in the model.

~~In JULES snow melting is caused by the sensible heat flux which is related to the temperature difference between the surface and the elevation level and the wind speed. Glaciers often have katabatic (downslope) winds which enhance the sensible heat flux and increase melting (Oerlemans and Grisogono 2002). It is important to represent the effects of katabatic winds on the mass balance when trying to model glacier melt, particularly at lower elevations where the katabatic winds speed is highest. To explicitly model katabatic winds would require knowledge of the gridbox mean slope at elevation bands, so instead a simple scaling of the surface wind speed is used to represent katabatic winds. Over glaciated grid boxes the wind speed is~~

$$\cancel{u_z = u_0 \gamma_{wind}}$$

~~(13)~~

~~where~~ $\cancel{\gamma_{wind}}$ ~~is a wind speed scale factor and~~ $\cancel{u_0}$ ~~is the surface wind speed. The simple scaling increases the wind speed relative to the surface forcing data and assumes that the scaling is constant for all heights.~~

2.2 Glacier ice albedo scheme

The existing spectral albedo scheme in JULES simulates the darkening of fresh snow as it undergoes the process of aging (Warren and Wiscombe, 1980). The growth rate of the grain is an empirically derived function of the snowpack temperature. The snow aging scheme does not reproduce the low albedo values typically observed on glacier ice, therefore a new albedo scheme is ~~it has been modified for~~ used ~~here~~. The new scheme is a density-dependent parameterization which was developed for the implementation in the Surface Mass Balance and Related Sub-surface processes (SOMARS) model (Greuell and Konzelmann, 1994). The scheme linearly scales the albedo from the value of fresh snow, to the value of ice, based on the density of the snowpack surface. The new scheme is used when the surface density of the top 10cm of the snowpack ($\rho_{surface}$) is greater than the firn density (550 kgm^{-3}) and the original snow aging scheme is used when ($\rho_{surface}$) is less than the firn density.

Formatted: Normal

$$\alpha_{\lambda} = \alpha_{\lambda,ice} + (\rho_{surface} - \rho_{ice})\left(\frac{\alpha_{\lambda,snow} - \alpha_{\lambda,ice}}{\rho_{snow} - \rho_{ice}}\right) \quad (14)$$

$\alpha_{\lambda,\ snow}$ is the maximum albedo of fresh snow, $\alpha_{\lambda,\ ice}$ is the albedo of melting ice, ρ_{snow} is the density of fresh snow (250 kgm^{-3}) and ρ_{ice} is the density of ice (917 kgm^{-3}). The albedo scaling is calculated separately in two radiation bands; visible wavelengths $\lambda = 0.3$–$0.7\mu m$ (VIS) and near-infrared wavelengths $\lambda = 0.7$–$5.0\mu m$ (NIR). The parameters, $\alpha_{vis,\ ice}$, $\alpha_{vis\ snow}$, $\alpha_{nir,\ ice}$, $\alpha_{nir,\ snow}$, γ_{temp}, γ_{precip} and γ_{wind} are tuned to obtain the best agreement between simulated and observed surface mass balance profiles for the present-day (see section 3).

2.3 Initialisation

The model requires initial conditions for (1) the snowpack properties (2) glaciated and unglaciated elevated tile fractions within a gridbox. The location of glacier grid points, the initial tile fraction and the present-day ice mass is set using data from the Randolph Glacier Inventory Version 6 (RGI6) (RGI Consortium, 2017). This dataset contains information on glacier hypsometry and is intended to capture the state of the world's glaciers at ~~s~~ the beginning of the 21st century. A new feature of the RGI6 is a 0.5-degree gridded glacier volume and area datasets, produced at 50m elevation bands. Volume was constructed for individual glaciers using an inversion technique to estimate ice thickness created using glacier outlines, a digital elevation model and a technique based on the principles of ice flow mechanics (Farinotti et al., 2009;Huss and Farinotti, 2012). The area and volume of individual glaciers have been aggregated onto 0.5-degree grid boxes. We bin the 50m area and volume into elevations bands varying from 0m to 9000m in increments of 250m to match the elevation bands prescribed in JULES.

2.3.1 Initial tile fraction

The elevated glaciated fraction is

$$frac_{ice(n)} = \frac{RGI\_area(n)}{gridbox\_area(n)} \quad (15)$$

where *RGI_area* is the area (km^2) at height from the RGI6, *n* is the tile elevation and *gridbox_area* (km^2) is the area of the gridbox. In this configuration of the model, any area that is not glaciated is set to a single unglaciated tile fraction ($frac_{rock}$) with a gridbox mean elevation. It is possible to have an unglaciated tile fraction at every elevation band, but since the glaciated tile fractions does not grow or shrink, we reduce our computation cost by simply putting any unglaciated area into a single tile fraction.

$$frac_{rock} = 1 - \sum_{n=1}^{n=nBands} frac_{ice}(n) \quad (16)$$

nBands = 37 is the number of elevation bands.

2.3.2 Initial snowpack properties

The snowpack is divided into ten levels in which the top nine levels consist of 5m of firn snow with depths [0.05m, 0.1m, 0.15m, 0.2m, 0.25m, 0.5m, 0.75m, 1m, 2m] and the bottom level has a variable depth. For each snowpack level the following properties must be set; density (kgm^{-3}), ice content (kgm^{-2}), liquid water content (kgm^{-2}), grain size (µm) and temperature (^{o}K). We assume there is no liquid content in the snowpack by setting this to zero. The density at each level is linearly scaled with depth, between the value for fresh snow at the surface (250kgm^{-3}), to the value for ice at the bottom level (917kgm^{-3}). ~~The ice content of the firn layers is calculated by multiplying the scaled density by the depth.~~

For the future simulations~~,~~ the thickness and ice mass at the bottom of the snowpack comes from thickness and volume data in the RGI6. The data is based on thickness inversion calculations from Huss and Farinotti (2012) for individual glaciers which are consolidated onto 0.5-degree gridboxes. The ice mass is calculated from the RGI6 volume assuming an ice density 917 kgm^{-3}. For the other layers the ice mass is calculated by multiplying the density by the layer thickness which is prescribed above. ~~ice content in the bottom level is set using the RGI6 volume assuming a constant ice density of 917kgm^{-3}. The depth of the bottom level is the ice content divided by the density.~~ For the calibration period, the ice mass at the start of the run (1979) is unknown. In the absence of any information about this, a constant depth of ~~5~~1000m is used which is selected to ensure that the snowpack never completely depletes over the calibration period. This consists of ~~4~~995m of ice at the bottom level of the snowpack and 5m of firn in the layers above. The ice content of the bottom level is the depth (9~~4~~95m) multiplied by the density of ice.

The snow grain size used to calculate spectral albedo (see section 2.2) is linearly scaled with depth and varies between 50µm at the surface for fresh snow to 2000µm at the base for ice. The snowpack temperature profile is calculated by spinning the model up for ~~one~~10 years for the calibration period and 1 year for the future simulations. ~~. The~~ The temperature at the top layer of the snowpack is set to the January mean temperature and the bottom layer and subsurface temperature is set to the annual mean temperature. For the calibration period the monthly and annual temperature comes from the last year of the spin-up. Setting the snowpack temperature this way ~~. This~~ gives a profile of warming towards the bottom of the snowpack representative of geothermal warming from the underlying soil. The initial temperature of the bedrock before the spin up is set to 0^{o}C but this adjusts to the climate as the model spins up~~when the model is spun up as part of the calibration procedure~~. We use these prescribed snowpack properties as the initial state for the calibration and future runs.

3 Mass balance calibration and validation

3.1 Model calibration

Elevation-dependent mass balance is calibrated for the present-day by tuning seven model parameters and comparing the output to elevation-band specific mass balance observations from the World Glacier Monitoring Service ((2017)~~[27](WGMS 2017, Global Glacier Change Bulletin No. 2 (2014-2015).)~~[27]~~(WGMS 2017, Global Glacier Change Bulletin No. 2 (2014-2015).)(WGMS 2017, Global Glacier Change Bulletin No. 2 (2014-2015).)~~(~~WGMS, (2017)~~. Calibrating mass balance against in-situ observations is a technique which has been used by other glacier modelling studies (Radić and Hock, 2011;Giesen and Oerlemans, 2013;Marzeion et al., 2012). For the calibration, annual elevation-band mass balance observations are used because there is data available for sixteen of the eighteen RGI6 regions. For validation, winter and summer elevation-band mass balance is used because there is less data available.

The tuneable parameters for mass balance are; visible snow albedo ($\alpha_{vis, snow}$), visible melting ice albedo ($\alpha_{vis, ice}$), near-infrared snow albedo ($\alpha_{nir, snow}$), near-infrared melting ice albedo ($\alpha_{nir, ice}$), orographic precipitation gradient (γ_{precip}), ~~dry adiabatic~~ temperature lapse rate (γ_{temp}) and wind speed scaling factor (γ_{wind}).

Random parameter combinations are selected using Latin Hyper Cube Sampling (McKay et al., 1979) between plausible ranges which have been derived from various sources outlined below. This technique randomly selects parameter values; however, reflectance in the VIS wavelength is always higher than in the NIR. To ensure the random sampling does not select NIR albedo values that are higher or unrealistically close to the VIS albedo values, we calculate the ratio of VIS to NIR albedo using values compiled by compiled by Roesch et al (2002) ~~et al., (2002)~~. The ratio VIS/NIR is calculated as 1.2 so any albedo values that exceed this ratio are excluded from the analysis. This reduces the sample size from 1000 to 198 parameter sets.

In the VIS wavelength the fresh snow albedo is tuned between 0.99 - 0.7 where upper bound value comes from observations of very clean snow with little impurities in the Antarctic (Hudson et al., 2006). The lower bound represents contaminated fresh snow and comes from taking approximate values from a study based on laboratory experiments of snow, with a large grain size (110 µm) containing 1680 parts per billion of black carbon (Hadley and Kirchstetter, 2012). Visible snow albedos of approximately 0.7 have also been observed on glaciers with black carbon and mineral dust contaminants in the Tibetan Plateau (Zhang et al., 2017). In the NIR wavelength the fresh snow albedo is tuned between 0.85 – 0.5 where the upper bound comes from spectral albedo observations made in Antarctica (Reijmer et al., 2001). We use a very low minimum albedo for melting ice (0.1) the VIS and NIR wavelengths to capture dirty debris covered ice.

The ~~dry adiabatic~~ temperature lapse rate is tuned between values of 4.0 – 10ºC km^{-1} where the upper limit is determined from physically realistic bounds and lower limit is from observations based at glaciers in Alps (Singh, 2001). The temperature lapse rate in JULES is constant throughout the year and assumes that temperature always decreases with height.

The wind speed scaling factor γ_{wind} is tuned within the range 1-4 to account for an increase in wind speed with height and for the presence of katabatic winds. The upper bound is estimated using wind observations made along the profile of the Pasterze glacier in the Alps during a field campaign (Greuell and Smeets, 2001). Table S6~~4~~ in the Supplementary Material contains the wind speed observations on the Pasterze glacier. The maximum observed wind speed was 4.6 ms^{-1} (at 2420 meters above sea-level) while the WATCH-ERA Interim dataset (WFDEI) (Weedon et al., 2014) surface wind speed for the same time period was 1.1ms^{-1} indicating a scaling factor of approximately 4.

The orographic precipitation gradient γ_{precip} is tuned between 5-25%/100m. This parameter is poorly constrained by observations therefore a large tuneable range is sampled. Tawde et al. (2016) estimated a precipitation gradient of 19%/100m for 12 glaciers in the Western Himalayas using a combination of remote sensing and in-situ meteorological observations of precipitation. Observations show that the precipitation gradient can be as high as 25%/100m for glaciers in Svalbard (Bruland and Hagen, 2002) while glacier-hydrological modelling studies have used much smaller values 4.3%/100m (Sorg et al., 2014) and ~~4.3~~3%/100m (Marzeion et al (2012). The tuneable parameters and their minimum and maximum ranges are listed in Table 1.

The model is forced with daily surface pressure, air temperature, downward longwave and shortwave surface radiation, specific humidity, rainfall, snowfall and wind speed from the WATCH-ERA Interim dataset (WFDEI) (Weedon et al., 2014). To reduce the computation time, only grid points where glacier ice is present are modelled. An ensemble of 198 calibration experiments are run. For each simulation the model is spun up for 10 years and the elevation-dependent mass balance is compared to observations at 149 fields sites over the years 197~~8~~9-2014.

The elevation-dependent mass balance observations come from stake measurements taken every year at different heights along the glaciers. Many of the mass balance observations in the WGMS are supplied without observational dates. In this case, we assume the mass balance year starts on the 1st October to ends on the 30th September with the summer commencing on the 1st May. Dates in the Southern hemisphere are shifted by six months. The observations are grouped according to standardised regions defined by the RGI6 (Fig. 2). The best regional parameter sets are identified by finding the minimum root mean square error between the modelled mass balance and the observations.

Figure 3 shows the modelled mass balance profiles plotted against the observations using the best parameter set for each region. The best regional parameter sets are listed in Table 2 and the root mean square error, correlation coefficient, Nash–Sutcliffe efficiency coefficient and mean bias are listed in Table 3. Nine out of the sixteen regions have a negative bias in the annual mass balance. Notably Svalbard, Southern Andes and New Zealand underestimate mass balance by 1 m.w.eq.yr^{-1}. The negative bias is also seen in the summer and winter mass balance and discussed in Section 3.2. ~~–The model can capture the accumulation and ablation rates reasonably well for many regions with the notable exception of the low latitude and Central European regions where melting is over estimated.~~

The model performs particularly poorly for the L~~l~~ow L~~l~~atitude region which has a large RMSE (3.02 m.w.eq.yr^{-1}). This region contains relatively small tropical glaciers in Colombia, Peru, Ecuador, Bolivia and Kenya. Marzeion et al (2012) found a poor correlation with observations in the low latitude region when they calibrated their glacier model using CRU data. They attributed that to the fact that sublimation was not included in their model, a process which is important for the mass balance of tropical glaciers. Our mass balance model ~~does~~ includes sublimation, so it is possible the WFDEI data over tropical glaciers is too warm. The WFDEI data is based on ERA-interim reanalysis where air temperature has been constrained ~~bias corrected~~

Formatted: Superscript

Formatted: Not Superscript/ Subscript

using CRU data. The CRU data comprises of temperature observations which are sparse in regions where tropical glaciers are located. Furthermore, the quality of the WFDEI data will depend on the performance of the underlying ECMWF model. ~~It is possible that the ECMWF model does not include glacier ice in tropical regions. The absence of ice to cool the lower atmosphere would make the grid box mean temperature too warm. In Central Europe the poor correlation with observations is predominantly caused by the Maladeta glacier in the Pyrenees (Fig. 4) which is a small glacier with an area of 0.52 km² WGMS (2017).~~ In Central Europe some of the poor correlation with observations is caused by the Maladeta glacier in the Pyrenees (Fig. 43) which is a small glacier with an area of 0.52 km^2 (WGMS, 2017). When this glacier is excluded from the analysis the correlation coefficient increases from 0.26 to 0.35 and the RMSE decreases from 2.03 to 1.73 meters of water equivalent per year.

3.2 Model validation

The calibrated mass balance is validated against summer and winter elevation-band specific mass balance for each region where data is available (Fig. ~~5~~4). ~~The model can reproduce the in-situ mass balance observations reasonably well considering the very coarse resolution of JULES in the horizontal (0.5-degree gridded) and vertical (250m increments) directions.~~ For all regions, except Scandinavia in the summer, negative Nash-Sutcliffe numbers are calculated for winter and summer elevation-dependent mass balance (Table 4). The negative numbers arise because the bias in the model is larger than the variance of the observations. There are negative biases for nearly all regions implying that melting is overestimated in the summer and accumulation is underestimated in the winter. This means that future projections of volume loss presented in section 4.2 might be overestimated.

The reason for the negative bias is because the model underestimates the precipitation and therefore the accumulation part of the mass balance is underestimated. This is because our approach to correcting the coarse scale gridded precipitation for orographic effects is simple. We use a single precipitation gradient for each RGI6 region and do not apply a bias correction. A bias correction is often recommended because precipitation is underestimated in coarse resolution datasets. Gauging observations are sparse in high mountains regions and snowfall observations can be susceptible to undercatch by 20–50% ~~(Rasmussen et al. 2012)~~(Rasmussen et al., 2012). Our precipitation rates are generally too low because we do not bias correct the precipitation.

Other studies use a bias correction that varies regionally ~~(~~(Radić and Hock, 2011;Radić et al., 2014;Bliss et al., 2014)~~Radic and Hock 2011, Radic et al. 2014, Bliss et al. (2014)~~. In those studies, the precipitation at the top of the glacier was estimated using a bias correction factor k_0. The decrease in precipitation from the top of the glacier to the snout was calculated using a precipitation gradient. To account for the fact that the mass balance of maritime and continental glaciers respond differently to precipitation changes k_0 was related to a continentality index. Our motivation for using a single precipitation gradient for each RGI6 region, and no bias correction was to test the simplest approach first, however the resulting biases suggest that this approach could be improved.

Formatted: Font: Not Italic

Formatted: Subscript

Formatted: Subscript

The impact of underestimating the precipitation is that we simulate negative mass balance in winter at some observational sites (Fig 5(A) and Fig 4.). To demonstrate this, we compare the mass balance components for two glaciers; the Leviy Aktru in the Russian Altai Mountains which has negative mass balance in the winter and Kozelskiy glacier in North Eastern Russia which has no negative mass balance in the winter (See Fig. S9). Both glaciers are in the North Asia RGI6 region, so have the same tuned parameters for mass balance. The simulated winter accumulation rates are much lower at Leviy Aktru glacier than Kozelskiy glacier leading to negative mass balance at the lowest 3 model levels below 2750m.

The simplistic treatment of the precipitation lapse rate also leads to instances where the model simulates positive mass balance in the summer at some locations (Fig 6 (A) and Fig 4.). We show the summer mass balance components for the same two glaciers in Fig S10. Positive mass balance is simulated at Kozelskiy glacier because accumulation exceeds the melting. This suggests that the precipitation gradient (19% per 100m for North Asia) is overly steep in the summer at this location.

Another reason we underestimate the accumulation ~~Some, but not all, of the bias~~ is due to the partitioning of rain and snow based on an air temperature threshold of 0^{o}C. The 0^{o}C threshold is likely too low, resulting in an underestimate of snowfall. When precipitation falls as rain or snow it adds liquid water or ice to the snowpack. The specific heat capacity of the snowpack is a function of the liquid water (W_k) and ice content (I_k) in each layer (k)

$$C_k = I_k C_{ice} + W_k C_{water} \qquad (17)$$

where C_{ice} = 2100 JK^{-1}kg^{-1} and C_{water} = 4100 JK^{-1}kg^{-1}. The liquid water content is limited by the available pore space in the snowpack, therefore changes in the snowfall (ice content) control the overall heat capacity. The underestimate in the ice content reduces the heat capacity which causes more melting than observed.

Other modelling studies have used higher air temperature thresholds; 1.5^{o}C (Huss and Hock 2015, Giesen and Oerlemans 2012), 2^{o}C (Hirabayashi et al 2010) and 3^{o}C (Marzeion et al 2012). An improved approach would use the wet-bulb temperature to partition rain and snow which would include the effects of humidity on temperature. Alternatively, a spatially varying threshold based on precipitation observations could be used. Jennings et al (2018) showed by analysing precipitation observations, that the temperature threshold varies spatially and generally higher ~~in~~for continental climates than ~~in~~ maritime climates. ~~. They found that the 50% rain-snow temperature defined as the temperatures above which precipitation is primarily snow, varied between maritime and continental climates.~~

W

~~Increasing the temperature threshold reduces the bias only slightly, therefore another explanation is that the precipitation in the WFDEI data is too low. Although we have included the variation in precipitation with height, if the gridbox mean precipitation is too low then snowfall on the elevated tiles will be underestimated. We did not bias correct the precipitation before applying the lapse rate correction unlike other studies do (Marzeion et al. 2012, Huss and Hock 2015).~~

Formatted: Superscript

Formatted: Superscript

Formatted: Subscript

Formatted: Subscript

Formatted: Subscript

Formatted: Superscript

Formatted: Superscript

Formatted: Subscript

Formatted: Superscript

Formatted: Superscript

Formatted: Superscript

Formatted: Superscript

Formatted: Superscript

~~Fig 5 and 6 shows the winter and summer mass balances for all observation sites when area thresholds of 100km2,300km2 and 500km2 are applied to the validation. The model predicts negative mass balance in winter and positive mass balance in summer at several sites (also seen in Fig. 4).~~

~~The negative mass balance in winter happens because the accumulation is underestimated and the positive mass balance in summer is when accumulation is overestimated.~~

~~To explore why we get negative winter mass balances we compare the mass balance components for two glaciers; the Leviy Aktru in the Russian Altai Mountains which has some melting in the winter and Kozelskiy glacier in North Eastern Russia which has no melting in the winter (See Fig. S9).~~

~~Both glaciers are in the North Asia RGI6 region, so have the same tuned parameters for mass balance; precipitation and temperature lapse rates, wind speed scaling and visible and near-infra albedos for snow and ice. The simulated accumulation rates are much lower at Leviy Aktru glacier than Kozelskiy glacier leading to negative mass balance at the lowest 3 model levels.~~

~~Our approach to the precipitation correction for height is very simple in contrast to other studies (Radic and Hock 2011, Radic et al. 2014, Bliss, Hock and Radic 2014). In those studies, the precipitation at the top of the glacier was estimated using a bias correction factor kp. The decrease in precipitation from the top of the glacier to the snout was calculated using a precipitation gradient. To account the fact the mass balance of maritime and continental glaciers respond differently to precipitation changes kp was related to a continentality index. This regional variation in the precipitation lapse as a function of climate is not included in our model. Neither do we include a bias correction factor meaning hat our acculination artes are too low.~~

~~The quality of the WFDEI precipitation maybe poor because the data is constrained by rain gauge observations which are sparse in high mountains regions and often biased towards low elevation levels. Even when observations are available snowfall at higher altitudes is often difficult to accurately measure and susceptible to undercatch by 20–50% (Rasmussen et al. 2012).~~

~~than winter.particularly~~

~~W~~inter mass balance is simulated better than summer mass balance, which is seen by the lower root mean square errors for winter in Table 4~~. For all observational sites, the model tends to overestimate the summer melting which can be seen in Fig. 7(A) and by the negative biases in Table 4.~~ . Furthermore, the biases are larger in the summer than in the winter (Table 4). It is likely that the simple albedo scheme, which relates albedo to the density of the snowpack surface, ~~does not~~ performs better in the winter when snow is accumulating than in summer when there is melting. ~~particularly well in the ablation zone.~~

Fig 5 (B-D) and Fig. 6 (B-D) shows the winter and summer mass balances for all observation sites when area thresholds of 100km^2, 300km^2 and 500km^2 are applied to the validation.

There is an improvement in the simulated summer mass balance when the glaciated area increases. This is seen by the improved correlation in Fig. ~~7~~6(D) in which the validation is repeated but only grid boxes with a glaciated area greater than

Formatted: Superscript

$500 km^2$ are considered. This indicates the~~at~~ ~~the~~ model is better a simulating summer ~~overestimation in~~ melting over ~~is more pronounced for small glaciated areas than~~ regions with a large ice extent, than over regions with a small glaciated area. ~~. The overestimate in melting in Central Europe is due mainly to the Maladeta glacier as discussed in Section 3.1.~~

4 Glacier volume projections

4.1 Downscaled climate change projections

Glacier volume projections are made for all regions, excluding Antarctica, for a range of high-end climate change scenarios. This is defined as climate change that exceeds 2ºC and 4ºC global average warming, relative to the pre-industrial period (Gohar et al., 2017). Six models fitting this criterion were selected from the Coupled Model Intercomparison Project Phase 5 (CMIP5). A new set of high resolution projections were generated using the ~~and downscaled using the~~ HadGEM3-A Global Atmosphere (GA) 6.0 model (Walters et al., 2017). ~~.~~ The sea surface temperature and sea-ice concentration boundary conditions for HadGEM3-A are supplied by the CMIP5 models. All models use the RCP8.5 'business as usual scenario' and cover a wide range of climate sensitivities~~itives~~, with some models reaching 2ºC global average warming relative to the pre-industrial period, quickly (IPSL-CM5A-LR) or slowly (GFDL-ESM2M) (Table 5). The models also cover a range of extreme wet or dry climate conditions. This is important to consider for glaciers in the central and eastern Himalaya which accumulate mass during the summer months due to monsoon precipitation (Ageta and Higuchi, 1984) and because future monsoon precipitation is highly uncertain in the CMIP5 models (Chen and Zhou, 2015).

The HadGEM3-A data are bias corrected using a trend preserving statistical bias method that was developed for the first Inter-Sectoral Impact Model Intercomparison Project (ISI-MIP) (Hempel et al., 2013). This technique uses WATCH forcing data (Weedon et al., 2011) to correct offsets in air pressure, temperature, longwave and shortwave downward surface radiation, rainfall, snowfall and wind speed but not specific humidity. The method adjusts the monthly mean and daily variability in the GCM variables but still preserves the long-term climate signal. ~~The native resolution of HadGEM3-A is N216 (~60km) which is suitable for capturing precipitation variability over complex topography.~~ The ~~data~~ HadGEM3-A was ~~was~~ bi-linearly interpolated from its native resolution of N216 (~60km), onto a 0.5-degree grid, to ~~fit~~match the resolution of the WATCH forcing data which was used for the bias correction. The daily bias corrected surface fields from the HadGEM3-A are used to run JULES offline to calculate future glacier volume changes. The bias correction was only applied to data up until the year 2097, which means the glaciers projections terminate at this year. A flow chart of the experimental set up is shown in Fig. ~~8~~7. The HadGEM3-A climate data was generated and bias corrected for the High-End cLimate Impact and eXtremes (HELIX) project.

4.2 Regional glacier volume projections 2011-2097

Glaciated areas are divided into 18 regions defined by the RGI6 with no projections made for Antarctic glaciers because the bias correction technique removes the HadGEM3-A data from this region. JULES is run for this century (2011 to 2097) using the best regional parameter sets for mass balance found by the calibration procedure (Table 2). No observations were available to determine the best parameters for Iceland and the Russian Arctic, therefore global mean parameter values are used for these regions. End of the century volume changes (in percent) are found by comparing the volume at end of the run (2097) to the initial volume calculated from the RGI6. Regional volume changes expressed in percent for low (0-2000m), medium (2250m-4000m) and high (4250m-9000m) and all elevation ranges (0-9000m) is listed in Table 6. The total volume loss over all elevation ranges is also listed in ~~in~~ mm of sea-level equivalent ~~are listed~~ in Table 6 and plotted in Fig. 1~~1~~0. Maps of the percentage volume change at the end of the century, relative to the initial volume are contained in the Supplementary Material in Figs. S1-S7~~6~~.

A substantial reduction in glacier volume is projected for all regions (Fig. ~~9~~8). Global glacier volume is projected to decrease by 64±5% by end of the century, where the value corresponds to the multi-model mean ± one standard deviation. The regions which lose more than 75% of their volume by the end of the century are; Alaska (-89 ± 2%), Western Canada and US (-100 ± 0%), Iceland (-98 ± 3%), Scandinavia (-98 ± 3%), Russian Arctic (-79 ± 10%), Central Europe (-99 ± 0 %), Caucasus (-100 ± 0 %), Central Asia (-80 ± 7%), South Asia West (-98 ± 1%), South Asia East (-95 ± 2 %), Low Latitudes (100 ± 0 %), Southern Andes (-98 ± 1%) and New Zealand (-88±5%). The HadGEM3-A forcing data shows these regions experience a strong warming. In most regions this is combined with a reduction in snowfall relative to the present day, which is drives the mass loss (Fig. 9~~10~~). Regions most resilient to volume losses are Greenland (-31 ± 5%) and Arctic Canada North (-47 ± 3%). ~~-~~In the case of Arctic Canada North snowfall increases relative to the present day which helps glaciers to retain their mass. There is a rapid loss of low latitude glaciers which has also been found by other global glaciers models (Marzeion et al., 2012;Huss and Hock, 2015). Our model overestimates the melting of these glaciers for the calibration period (Fig. 3), so this result should be treated with a degree of caution.

~~The percentage volume changes for three different elevation ranges; low (0-2000m), medium (2250m-4000m) and high (4250m-9000m) are listed in Table 6.~~ Some of the high latitude regions particularly Alaska, Western Canada & US, Svalbard and North Asia experience very large volume increases at their upper elevation ranges. This would be reduced if the model included glacier dynamics, because ice would be transported from higher elevations to lower elevations.

The ensemble mean global sea level equivalent contribution is 215.2 ± 21.3 mm. The largest contributors to sea~~-~~-level rise are Alaska (44.6 ± 1.1mm), Arctic Canada North and South (34.9 ± 3.0mm), Russian Arctic (33.3 ± 4.8mm), Greenland (20.1±4.4), High Mountain Asia (combined Central Asia, South Asia East and West), (18.0 ± 0.8mm), Southern Andes (14.4 ± 0.1mm) and Svalbard (17.0 ± 4.6mm). These are the regions which have been observed by the Gravity Recovery and Climate Experiment (GRACE) satellite to have lost the most mass in the recent years (Gardner et al., 2013).

To investigate which parts of the energy balance are driving the future melt rates, we show the energy balance components averaged over all regions and all elevation levels in Figure 11~~Fig. 11~~. Future melting is caused by a positive net radiation of approximately 30 Wm^{-2} that is sustained throughout the century. This is comprised of 18 Wm^{-2} net shortwave, 3 Wm^{-2} net longwave, 5 Wm^{-2} latent heat flux and 4 Wm^{-2} sensible heat flux. The largest component of the radiation for melting comes from the net shortwave radiation. The upward shortwave radiation comprises of direct and diffuse components in the visible and near infrared wavelengths. The visible albedo deceases because melting causes the ice surface to darken. In contrast, the near infrared albedo increases because the ice is heating up emitting radiation in the infrared part of the spectrum.

The downward and upward longwave radiation are increasing in future however, the net longwave radiation contribution to the melting is small. The downward longwave radiation increases because of the T^4 relationship with air temperature, whereas the upward longwave radiation increases because the glacier surface is warming. The latent heat flux from refreezing of melt water and the sensible heat from surface warming, are also small components of the net radiation balance.

4.3 Mass Balance Components

In this section we examine how the surface mass balance components vary with height and how this will change in the future. Figure 12~~Figure 12Figure 12~~ shows the accumulation, refreezing and melting contributions to mass balance averaged over low, medium and high elevations ranges for the period 1980-2000. Sublimation is excluded because its contribution to mass balance is relatively small. As ~~expected~~expected, there is more melting ~~As expected melting increases towards~~ in the lower elevation~~s~~ ranges and more ~~more a~~accumulation ~~increases towards~~at the higher elevation ranges. ~~s.~~

The refreezing component, which includes refreezing of melt water and elevated adjusted rainfall, shows no clear variation with height~~discernible pattern~~. – This is because the refreezing component can both increase and~~or~~ decrease ~~at lower elevations~~with height. ~~It~~Refreezing can -increases towards lever elevations ~~The~~because there is more rain and melted water. It can also decrease~~s~~ if the s~~there is no s~~nowpack is depleted or if there is not enough pore space to hold water ~~-refreezing component increases at lower elevation are there is more rainfall and melt water. The refreezing component decrease towards lower elevations because the under warm conditions snowpack might disappear or under cool conditions there there is no pore space to hold water~~ because previous refreezing episodes have converted the firn into solid ice. The largest accumulation rates occur in Alaska (5.3 m.w.eq.yr^{-1}) –and Western Canada and US (7.3 m.w.eq.yr^{-1}) ~~for the~~between ~~high~~ 4250m-9000m and the ~~elevation range.~~largest melt rates are found in the Caucasus and Middle East (-7.4 m.w.eq.yr^{-1}) and the Low Latitudes (-7.6 m.w.eq.yr^{-1}).

-Figure 13~~Figure 13Figure 13~~ shows how the global annual mass balance components vary with time for low, medium and high elevations ranges.

There is a reduction in accumulation and refreezing at all elevation ranges towards the end of the century. Melt rates decreases at medium and high elevation ranges because glaciers mass is lost at these altitudes, therefore less ice is available to melt (see Fig. S8 for the future cumulated mass balances ~~distribution of ice volume~~ as a function of height). Melt rates are constant at the low elevation ranges because there remains substantial quantities of ice available to melt at the end of the ~~C~~century in Greenland, Arctic Canada North and South, Svalbard, Russian Arctic. ~~There is a reduction in ma~~At high elevations mass balance is reduced from -2.2 m.w.eq.yr^{-1} (-177 Gtyr^{-1}) during the historical period (1980–2000) to -0.35 m.w.eq. yr^{-1} (-28 Gtyr^{-1}) by~~by,~~ the end of the century (2080-2097). Similarly, for the medium elevation ranges mass balance reduces from -0.56 m.w.eq.yr^{-1} (-26 Gtyr^{-1}) to -0.24 m.w.eq.yr^{-1} (-11 Gtyr^{-1}).

Formatted: Superscript

Formatted: Superscript

Formatted: Superscript

Formatted: Not Superscript/ Subscript

Formatted: Not Superscript/ Subscript

Formatted: Not Superscript/ Subscript

Formatted: Not Superscript/ Subscript

Formatted: Not Superscript/ Subscript

Formatted: Not Superscript/ Subscript

4.4 Parametric uncertainty analysis

The standard deviation in the volume losses presented above are relatively small. This is because only a single GCM was used to downscale the CMIP5 data (HadGEM3-A). The uncertainty in the ensemble mean reflects the impact of the different sea-surface temperature and sea-ice concentration boundary conditions, provided by the CMIP5 models, on the HadGEM3-A climate. Other sources of uncertainty in the projections can arise from the calibration procedure, observational error, initial glacier volume and area, and structural uncertainty in the model physics. It is beyond the scope of this paper to investigate all the possible sources of uncertainty on the glacier volume losses. Instead we discuss the impact of parametric uncertainty in the calibration procedure in the following section.

In the calibration procedure the mass balance was tuned to obtain an optimal set of parameters for each RGI6 region, however, there may be other plausible parameter sets that perform equally well (i.e. for which the RMSE between the observations and the model is small). The principle of 'equifinality', in which the end state can be reached by many potential means, is important to explore because some parameters may compensate for each other. For example, the same mass balance could be reached by increasing the wind scale factor which enhances melting or decreasing the precipitation gradient which would reduce accumulation. To identify the experiments that perform equally well, we identify where there is a step change in the gradient of the RMSE for each RGI6 region. A similar approach was used by Stone et al. (2010)~~Stone et al. (2010)~~ to explore the uncertainty in the thickness, volume and areal extent of the present-day Greenland ice sheet from an ensemble of Latin Hypercube experiments. The step change in the RMSE is identified using the changepoint detection algorithm called findchangepts (Rebecca et al., 2012;Lavielle, 2005) from the MATLAB signal processing toolbox. The algorithm is run to find where the mean of the top ten experiments (excluding the optimal experiment) changes the most significantly. For each RGI6 region the step changes in the RMSE are shown in Fig. 1~~2~~4~~3~~.

JULES is re-run for each of the downscaled CMIP5 experiments and for each parameter set that is defined as performing equally well (See Table S1 in the Supplementary Material for a list of the parameters sets that perform equally well). The volume losses expressed in mm of sea-level equivalent are shown in Fig. 154~~3~~. The effects of the parametric uncertainty on the volume losses varies regionally, with the largest impact found for Central Europe and Greenland. Regional volume loses including parametric uncertainty in the calibration are summarised in Table 7. Including calibration uncertainty in this way ~~Including parametric uncertainty does not change the multi-model mean global volume loss substantially but it does increase the uncertainty range (Fig. 14). This~~ gives an upper bound of 247.3 mm sea-level equivalent volume loss by the end of the century.

Another way to explore the uncertainty in the volume projections caused the calibration procedure, is to use different performance metrics to identify best parameters sets. In addition to using RMSE, we calculate best parameter sets by (1) minimising the absolute value of the bias and (2) maximizing the correlation coefficient. The best regional parameter sets are different depending on the choice of performance metric used (See Tables S2 and S3 in the Supplementary material). For twelve regions, minimising the bias results in higher precipitation lapse rates, than when RMSE values are used to select parameters. This suggests the bias in many regions is caused by underestimating the precipitation lapse rates. As discussed above, this could be due to the fact the gridbox mean WFDEI precipitation was not bias corrected. Glacier volume projections are generated by repeating the simulations using these two additional performance metrics to identify best parameter sets. The uncertainty in the global volume loss when the extra performance metrics are used, is approximately double the uncertainty arising from the different climate forcings ~~Including parametric uncertainty does not change the multi-model mean global volume loss substantially but it does increase the uncertainty range~~ (Fig. 1~~46~~6~~5~~, Table 7). When extra performance metrics are used, the upper bound volume loss increases to 281.1 mm sea-level equivalent by the end of the century.

4.5 Comparison with other studies

We compare our end of the century volume changes (excluding parametric uncertainty), to two other published studies which used the CMIP5 ensemble under the RCP8.5 climate change scenario (Huss and Hock, 2015;Radić et al., 2014). Other studies exist, but these include the volume losses from Antarctic glaciers which makes a direct comparison difficult (Marzeion et al., 2012;Slangen et al., 2014;Giesen and Oerlemans, 2013;Hirabayashi et al., 2013). Huss and hock (2015) listed regional percentage volume change and sea-level equivalent values in their study while Radić ~~Radic~~ et al. (2014) listed sea-level equivalent~~eqiuivalent~~ values only (See the comparison Tables S4~~2~~ and S5~~3~~ in the Supplementary material).

Our end of the century percentage volume losses compare reasonably well to Huss and Hock (2015) for Central Europe, Caucasus, South Asia East, Scandinavia, Russian Arctic, Western Canada and US, Arctic Canada North, North Asia, Central Asia, L~~l~~ow ~~l~~Latitudes and New Zealand but are significantly higher in the Southern Andes, Alaska, Iceland and Arctic Canada South. The uncertainty in our percentage volume losses are smaller than Huss and Hock (2015) because we only use a single GCM to downscale the CMIP5 experiments while Huss and Hock (2015) use 14 CMIP5 GCMs.

We estimate the end of century global sea-level contribution, excluding Antarctic glaciers, to be 215 ± 20mm which is higher than 188mm (Radić et al., 2014) and 136±23mm (Huss and Hock, 2015) caused mainly by greater contributions from Alaska, Southern Andes and the Russian Arctic. These three regions are discussed in turn.

For the Southern Andes our estimates are approximately double (14.4mm) that of the other studies (5.8mm (Huss and Hock, 2015), 8.5mm (Radić et al., 2014)). This region has the largest negative bias in the calibrated present-day mass balance (-2.87 m.w.eq.yr^{-1} see Table 3). To explore the effects of correcting the calibration bias on the ice volume projections, we subtract the bias values listed in Table 3 from the future annual mass balance rates. Each gridbox is assumed to have the same regional mass balance bias. The bias corrected volume losses are listed in Table S5 in the supplementary material. For the Southern Andes, the volume losses are much closer to the other studies (7.6mm) when the bias is corrected. The impact is less for the other regions where the biases are smaller. For the Russian Arctic our volume losses are higher than the other studies but that should be interpreted with caution because there were no observations available in this region to get a tuned parameter set (global mean parameters where used instead). In Alaska the bias in annual mass balance is small (0.06 m.w.eq.yr^{-1}) so correcting the bias has little effect on the volume loss projection for this region.

Applying the bias correction increases the global volume loss from 215 ± 20mm to 223 ± 20 mm, therefore the difference between our model and the other studies cannot be explained by the bias in the calibration.

~~global bias is 0.19 207.8±20.3mm is still higher than the other studies. For Alaska the bias is very small~~

It is likely that our SLE contributions are higher than the other studies because the climate forcing data is different. ~~It is unsurprising that our SLE contributions are higher than the other studies because t~~The HadGEM3-A model uses boundary conditions from a subset of RCP8.5 ~~the~~ CMIP5 models with the highest warming levels. Furthermore, the HadGEM3-A data has a higher resolution (approximately 60km) than the CMIP5 data which was used by the other two studies. This means our model should, in theory, be more accurate at reproducing regional patterns in precipitation and temperature over complex terrain which is important for calculating mass balance.

~~Another explanation why we predict more volume loss than Radic et al. (2014) and Huss and Hock (2015) is because there is no retreat of the glacier terminus represented in the model. The only way for glaciers to reach equilibrium with climate is by melting completely. A study by Marzeion et al. (2014) showed that models predict more mass loss when the terminus elevation is fixed than when it is allowed to vary. This is because when the terminus is allowed to retreat, there will be less area available to melt. Marzeion et al found that neglecting terminus elevation changes resulted in an extra few tens of mm SLE depending on RCP scenario.~~

~~Another difference is that we consolidate individual glaciers into a coarse gridbox and do not model glacier dynamics. In contrast, the other studies model the dynamics of individual glaciers using an elevation change parameterisation (Huss and Hock 2015) or volume-area scaling (Radic et al. 2014). The effect of not including ice flow in our model is that large glaciers will accumulate mass at high elevations because there is no transport of mass to lower elevations. Furthermore, the mass at low elevations will melt too quickly because ice is not replaced by ice flow. Including ice flow would increase the volume loss, because ice would be transported from higher to lower elevations where the temperatures are warmer. For this reason, we assume that excluding ice flow does not explain why our volume losses are higher than the other studies. Lastly, some of the differences between our study and other published projections could be due models using different the method used to initialise the present-day ice volumes and glaciated areas.~~

5 Discussion

The robustness of the glacier projections depends on how well the model can reproduce present-day glacier mass balance. Our calibrated seasonal mass balance contains a negative bias (accumulation is underestimated, and melting is overestimated) which suggests the projections of volume loss might be overestimated. One of the main shortcomings of the calibration and validation of mass balance is that only a single type of observations is used. This data was used because we wanted to ensure the model could reproduce variations in accumulation and ablation with height when the elevated tiling scheme was introduced. Point mass balance observations are affected by local factors such as aspect, avalanching, debris cover and there is a possibility that these local factors affect parameter sets chosen for entire RGI region. This could be improved by using observations from satellite gravimetry and altimetry, such as that described by Gardner et al (2013) to get a quantitative estimate of the model performance at the regional scales.

~~mass balance ,~~.One of the notable differences between our study and other global glacier models is that our tuned precipitation lapse rates are very high, for example, 24%/100m for South Asia West and 19%/100m for Central Asia. Other models have used lower precipitation lapse rates (1-2.5%/100m (Huss and Hock, 2015), 3%/100m (Marzeion et al., 2012)), but they also bias correct precipitation by multiplying by a scale factor. This scaling factor can be considerably high. Giesen and Oerlemans (2012) found that precipitation needed to be multiplied by a factor of 2.5 to get good agreement with mass balance observations. Radić ~~Radic~~ and Hock (2011) derived, through calibration of present-day mass balance, a precipitation scale factor of as high as 5.6 for Tuyuksu and Golubina glaciers in the Tien Shan. Our lapse rates are high because we do not bias correct the precipitation using a multiplication factor for the present-day. For the future GCM data the gridbox mean precipitation was bias corrected using the ISI-MIP technique. The negative bias that we get when validating the present-day mass balance suggests that snowfall is underestimated in our model. A future study using this model could test whether bias correcting the precipitation before applying the lapse rate correction improves the simulated mass balance.

This is the first attempt to implement a glacier scheme into JULES and so the model has many limitations. One of the key shortcomings is that glacier dynamics is not included (glacier area does not vary). The transport of ice from ~~The model does not simulate the retreat of the glacier terminus which results in an overestimate of mass loss. Neither does the model simulate the transport of ice from~~ higher elevations to lower elevations is not included. This~~ese~~ process~~es~~ could be included in future work by adding a

~~There are several avenues for future model development. Firstly, glacier dynamics in not currently included in the model. Ice flow could be included using a~~ volume-area scaling scheme Bahr~~-~~ (1997) or a thickness parameterisation based on glacier slope (Marshall and Clarke, 2000). – Volume-area scaling has been used to model glacier dynamics in coarse resolution (0.5-degree) models where all glaciers in a gridbox are represented by a single ice body (Kotlarski et al., 2010;Hirabayashi et al., 2010). The current configuration of elevated glaciated and unglaciated tiles in JULES makes it well suited to a volume-area scaling model. This would be implemented by growing (shrinking) the elevated glaciated tiles if mass balance is positive (negative) at each elevation band. In the case where the elevated ice tile grows the unglaciated tile would shrink at that elevation band or vice versa.

The volume-area scaling law has been used successfully to model the dynamics of individual glaciers (Radić et al., 2014;Giesen and Oerlemans, 2013;Marzeion et al., 2012;Slangen et al., 2014) but has some limitations when applied to coarse models where glaciers are consolidated into a single gridbox. The volume-area scaling law, relates volume to area using a constant scaling exponent which is typically derived from a small sample of glacier observations (Bahr et al., 1997). One of the draw backs is that the law is non-linear, meaning the exponent derived from individual glaciers would overestimate the volume of a large ice grid box such as in our model (Hirabayashi et al., 2013). Furthermore, the exponent may not accurately represent the volume-area relationship in other geographical regions. To overcome these issues a spatially variable scaling exponent could be created using the newly available 0.5-degree data on volume and area contained in the RGI6.

Another limitation of the model, which may be problematic for same applications, is that the gridbox mean precipitation is not conserved when precipitation is adjusted for elevation. This correction was necessary to get enough accumulation in the mass balance at high elevations. One way to conserve water mass would be to reduce the precipitation onto the non-glaciated area of the grid cell. This would represent horizontal mass movement within the grid box from wind-blown snow and avalanching.

A further~~n~~ limitation~~other shortcoming~~ of the model is the simple treatment of katabatic winds, which is modelled by scaling the synoptic wind speed. ~~A secondly avenue for model development could focus on the treatment of katabatic winds in the model. We represent katabatic winds by simply scaling of the surface wind speed.~~ This could be improved by parameterising katabatic winds based on the gridbox slope and the temperature difference between the glacier surface and the air temperature using the Prandtl model (Oerlemans and Grisogono 2002).

Another ~~additional~~ drawback of the model is the coarse resolution of the gridboxes which make it unfeasible to include some process which affect local mass balance such as hillside shading, avalanching, blowing snow and calving. The model could, however, be run on a finer resolution using higher resolution climate forcing data.

~~There are limitations to the processes that can feasibly be modelled in such a coarse resolution model. For example, avalanching, blowing snow and calving are important processes that affect the local mass balance but would pose a challenge to model on a coarse resolution grid. Finally, w~~While this modelling projects considerable reduction in glacier mass ~~balance~~ for all mountain ranges by the end of this century, it is clear that many of the world's mountain glaciers will evolve in ways that are currently difficult to model. For instance, paraglacial processes during deglaciation lead to enhanced rock falls and debris flows from deglaciating mountain slopes and these deliver rock debris to glacier surfaces. This produces debris-covered glaciers and these are common in many mountain regions, including in Alaska, arid Andes, central Asia and in the Hindu Kush-Himalaya. Thick debris cover (decimetres to metres) limits ice ablation, (e.g., (Lambrecht et al., 2011;Pellicciotti et al., 2014;Lardeux et al., 2016;Rangecroft et al., 2016)) and reverses the mass balance gradient, with comparatively higher ablation rates up glacier than at the debris-covered terminus. This significantly influences glacier dynamics (Benn et al., 2005), and with inefficient sediment evacuation eventually leads to the transition from debris-covered glaciers to rock glaciers (e.g (Monnier and Kinnard, 2017). In the context of continued climate warming, the transition from ice glaciers to rock glaciers may enhance the resilience of the mountain cryosphere (Bosson and Lambiel, 2016). As a result, better assessment of the response of the mountain cryosphere to climate warming will depend on a clearer understanding of glacier-rock glacier relationships.

There are three key strengths to the JULES glacier model. Firstly, we include variations in orography within a climate gridbox which is important to calculate elevation-dependent glacier mass balance. Kotlarski et al (2010) developed a glacier scheme for the REMO regional climate model by lumping glaciers into 0-5-degree gridboxes in a similar approach to us, but they did

Formatted: Font: Not Italic

not have a representation of subgrid orography. Instead glacier gridboxes received double the gridbox mean snowfall, glacier ice had a fixed albedo and a constant lapse rate was applied to adjust temperatures. They concluded that to reproduce mass balance trends over the Alps, the scheme needed to include subgrid variability of atmospheric parameters within a gridbox. Secondly, the model uses a full energy balance scheme to calculate glacier melting. This is a more physically based approach than the widely used temperature index models, which relate melting to temperature using a degree day factor (DDF). The DDF lumps all the energy balance components into a single number meaning that the effects of changing wind speed, cloudiness and radiation on melt rates cannot be considered. Changes in solar radiation can be an important driver of melting. Huss et al (2009) studied long term mass balance trends for a site in the Alps and showed that melting was stronger during the 1940's than in recent years despite more warming. This was because summer solar radiation was higher during the 1940s. Moreover, temperature index models have been found to be less accurate with increasing temporal resolution (for example on daily time steps) (Hock, 2005). In this paper, we present a brief analysis of the future global energy balance fluxes, but how the fluxes vary for individual regions and elevation levels could be investigated further. -Finally, the glacier scheme is coupled to a land surface model, which presents opportunities for further studies. For instance, the model could be used to investigate the impact of climate change on river discharge in glaciated catchments in Asia, South America or the Arctic.

6 Conclusions

The first aim of this study was to add a glacier component to JULES to develop a fully integrated model, to simulate the interactions between glacier mass balance, river runoff, water abstraction by irrigation and crop production. To do this we added two new surface types to JULES; elevated glaciated and unglaciated tiles. This allows us to the calculate elevation-dependent mass balance which can be used to study the response of glaciers to climate change. Glacier volume was modelled by growing or shrinking the snowpack, using the elevation-dependent mass balance, but glacier dynamics was not included. Present-day mass balance was calibrated by tuning albedo, wind speed, temperature and precipitation lapse rates to obtain a set of regionally tuned parameters which are then used to model future mass balance. Winter and summer mass balances are reproduced reasonably well for regions where the glaciated area is large, however, the model performs poorly for small glaciers particularly in the summer. The fully integrated model is potentially a useful tool for the scientific community to study the impact of climate change on food and water resources.

The second aim of this study was to make glacier volume projections for the future under a range of high-end climate change scenarios. The ensemble mean volume loss ± one standard deviation is, -64±5% for all glaciers excluding those on the periphery~~peripheral~~ of the Antarctic ice sheet. The small uncertainties in the multi-model mean are caused by the sensitivity of HadGEM3-A to the boundary conditions supplied by the CMIP5 models. Our end of the century global volume loss is 215 ± 20mm, which is higher than values reported by other studies. This is because we used a subset of CMIP5 models with the highest warming levels to drive the model and glacier dynamics is not included which results in more mass loss than other studies that include dynamics. Including parametric uncertainty in the calibration procedure results in an upper bound global volume loss of 281.1 mm sea-level equivalent by the end of the century. The projected ice losses will have an impact on sea-level rise and on water availability in glacier-fed river systems.

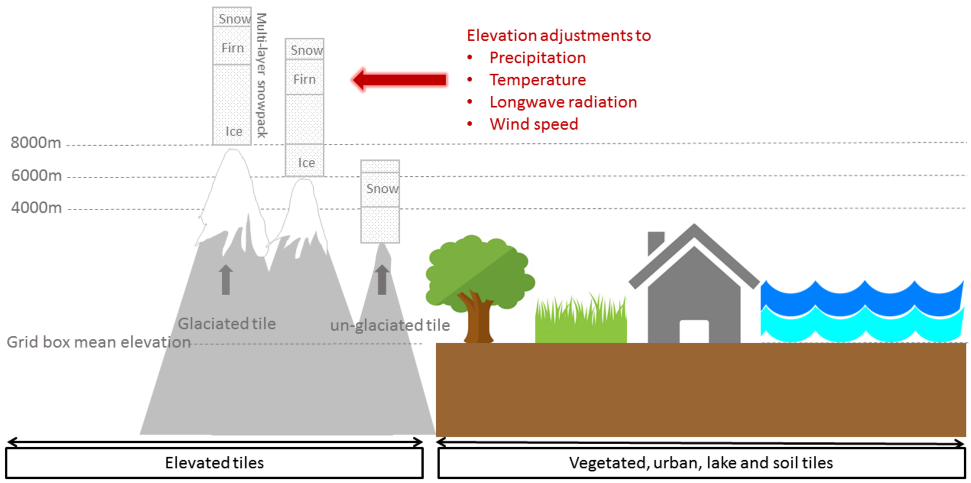

Figure 1 Schematic of JULES surface types inside a single gridbox. The new elevated glaciated and unglaciated tiles are shown on the left-hand side. Note that elevated glaciated and unglaciated tiles are not allowed to share a gridbox with the other tiles.

Table 1 Tuneable parameters for mass balance calculation and their ranges from the literature

Parameter	*Range of values*	*Symbol*	*Units*
Fresh snow albedo (VIS)	0.99 - 0.7	$\alpha_{vis,\ snow}$	-
Fresh snow albedo (NIR)	0.85 - 0.5	$\alpha_{nir\ snow}$	-
Ice albedo (VIS)	0.7 – 0.1	$\alpha_{vis,\ ice}$	-
Ice albedo (NIR)	0.6 – 0.1	$\alpha_{nir,\ ice}$	-
Temperature lapse rate	4 – 9.8	γ_{temp}	^{o}K km^{-1}
Orographic precipitation gradient	5 – 25	γ_{precip}	%/100m
Wind speed scale factor	1 - 4	γ_{wind}	-

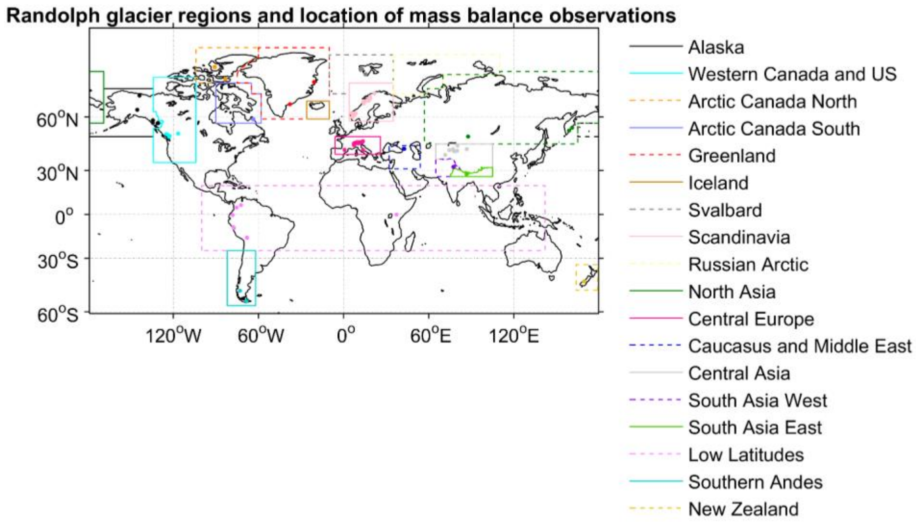

Figure 2: The location of mass balance profile observations glaciers from the World Glacier Monitoring Service and the Randolph Glacier Inventory regions (version 6.0)

Formatted: Caption, Line spacing: 1.5 lines

Table 2 Best parameter sets for each RGI6 region. The regions are ranked from the lowest to the highest RMSE. There are no observed profiles for Iceland and Russian Artic, so the global mean parameters values are used (bold) for the future simulations

Region	$\alpha_{vis,snow}$	$\alpha_{nir,snow}$	$\alpha_{vis,ice}$	$\alpha_{nir,ice}$	γ_{temp} $^oK\ km^{-1}$	γ_{precip} *%/100m*	γ_{wind}
Arctic Canada South	0.94	0.77	0.68	0.53	8.3	16	2.15
Arctic Canada North	0.96	0.70	0.49	0.12	4.2	7	1.10
Greenland	0.95	0.72	0.41	0.19	8.0	15	1.07
Alaska	0.88	0.65	0.56	0.27	8.2	16	1.32

South Asia East	0.91	0.73	0.67	0.56	5.3	9	1.55
South Asia West	0.99	0.73	0.60	0.30	4.0	24	1.69
Western Canada and US	0.97	0.64	0.45	0.26	9.3	8	2.29
Central Asia	0.94	0.74	0.69	0.50	8.1	19	1.40
North Asia	0.94	0.74	0.69	0.50	8.1	19	1.40
Central Europe	0.83	0.63	0.59	0.35	5.8	7	1.83
Svalbard	0.95	0.76	0.54	0.35	9.0	14	1.02
Caucasus and Middle East	0.90	0.71	0.53	0.28	8.3	5	3.32
Scandinavia	0.95	0.76	0.54	0.35	9.0	14	1.02
New Zealand	0.94	0.74	0.69	0.50	8.1	19	1.40
Low Latitudes	0.94	0.74	0.69	0.50	8.1	19	1.40
Southern Andes	0.95	0.76	0.54	0.35	9.0	14	1.02
Mean	**0.93**	**0.72**	**0.58**	**0.37**	**7.55**	**14**	**1.56**

Table 3 Root mean square error (RMSE), correlation coefficient (r), Nash–Sutcliffe efficiency coefficient (NS), mean bias (BIAS) and the number of elevation-band mass balance observations (No Obs) for RGI6 regions. The regions are ranked from the lowest to the highest RMSE.

Region	*RMSE* *m.w.eq.yr^{-1}*	*r*	*NS*	*Bias* *m.w.eq.yr^{-1}*	*No Obs*
Arctic Canada South	0.96	0.61	0.11	0.10	72
Arctic Canada North	1.06	0.19	-0.44	0.52	1,332
Greenland	1.09	0.66	0.14	0.14	90
Alaska	1.36	0.65	0.38	0.06	217
South Asia East	1.41	0.15	-0.34	-0.19	81
South Asia West	1.53	0.62	0.38	-0.09	168
Western Canada and US	1.73	0.69	0.41	-0.40	916
Central Asia	1.81	0.22	-1.15	-0.51	2,519

North Asia	1.95	0.45	-0.04	-0.21	1,335
Central Europe	2.03	0.26	-0.65	0.30	9,561
Svalbard	2.16	0.36	-6.86	-1.21	1,647
Caucasus and Middle East	2.23	0.30	-0.89	0.33	687
Scandinavia	2.40	0.53	0.20	0.67	10,617
New Zealand	2.57	0.58	-0.30	-1.09	45
Low Latitudes	3.06	0.36	-0.71	-0.88	1,016
Southern Andes	3.33	0.26	-12.33	-2.87	118
Global	2.16	0.40	-0.11	0.19	30,421

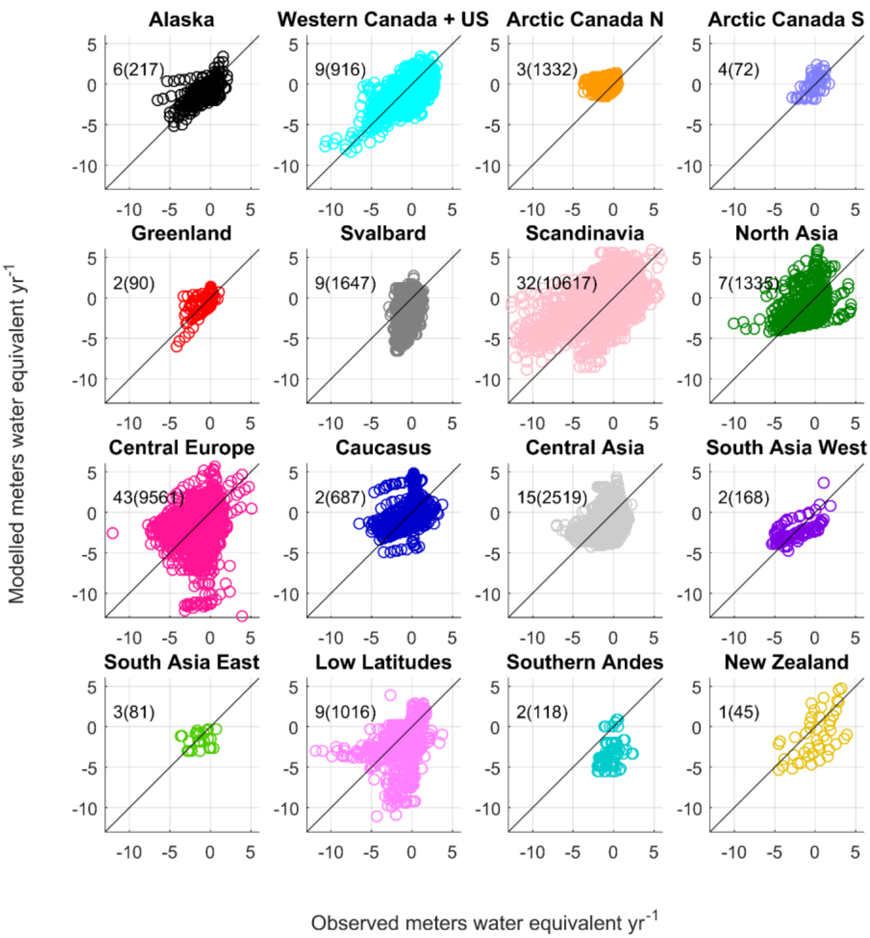
Alaska
Western Canada + US
Arctic Canada N
Arctic Canada S
Greenland
Svalbard
Scandinavia
North Asia
Central Europe
Caucasus
Central Asia
South Asia West
South Asia East
Low Latitudes
Southern Andes
New Zealand
6(217)
9(916)
3(1332)
4(72)
2(90)
9(1647)
32(10617)
7(1335)
43(9561)
2(687)
15(2519)
2(168)
3(81)
9(1016)
2(118)
1(45)
Modelled meters water equivalent yr-1
Observed meters water equivalent yr-1

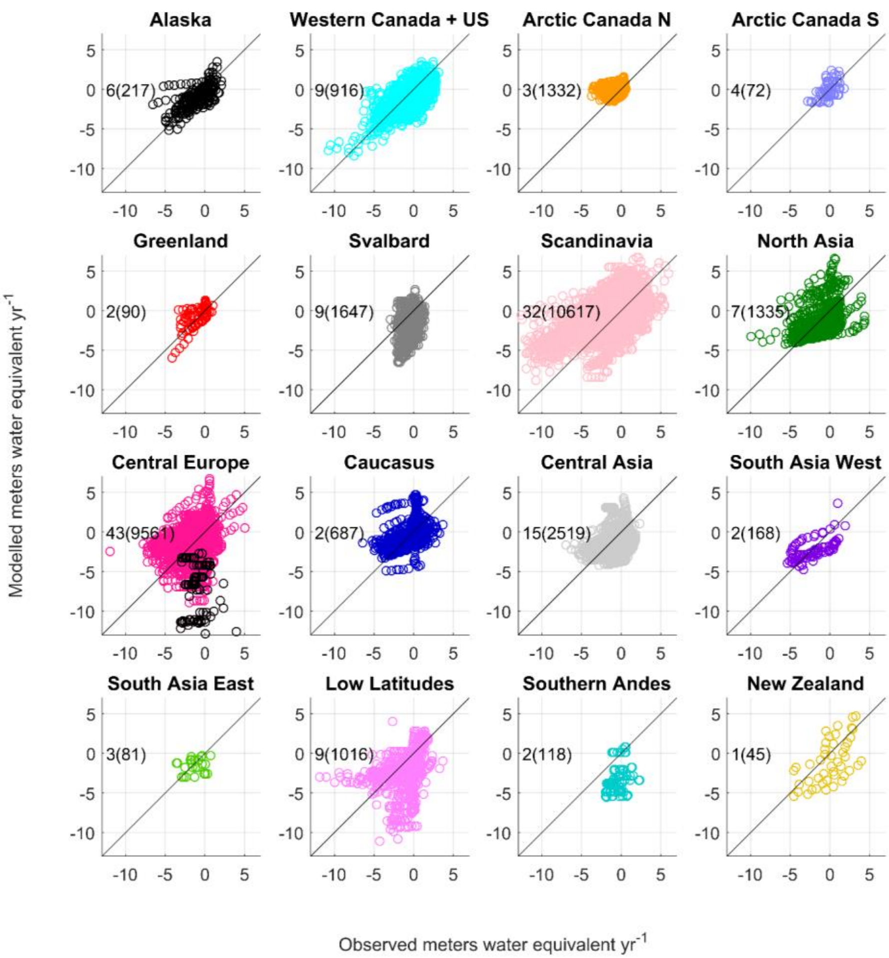

Figure 3~~:~~ Modelled annual elevation-dependent specific mass balance against observations from the WGMS. The modelled mass balance is simulated on a 0.5-degree grid resolution at 250m elevation bands and the observations are for individual glaciers at elevation levels specific to each glacier. The observed mass balance is interpolated onto the JULES elevation bands. If only a single observation exists, then mass balance for the nearest JULES elevation band is used. The number of glaciers is shown in the top left-

hand corner and the number of observation points in brackets. **In central Europe mass balance for the Maladeta glacier in the Pyrenees is shown in black circles.**

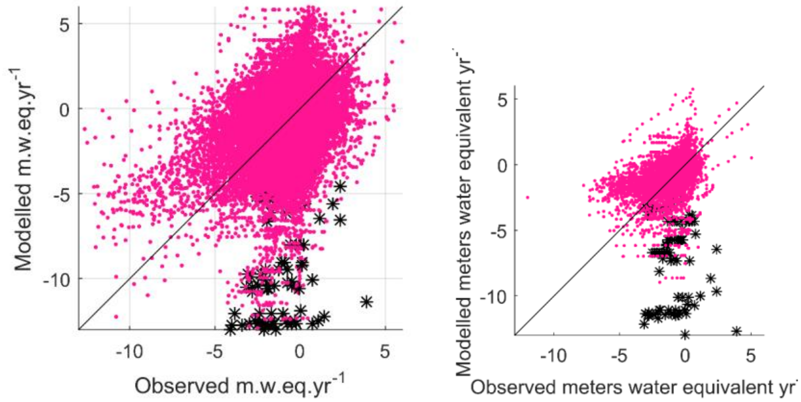

~~**Figure 4: Modelled and observed mass balance profiles for Central Europe (dots) and Maladeta glacier in the Pyrenees (asterixis).**~~

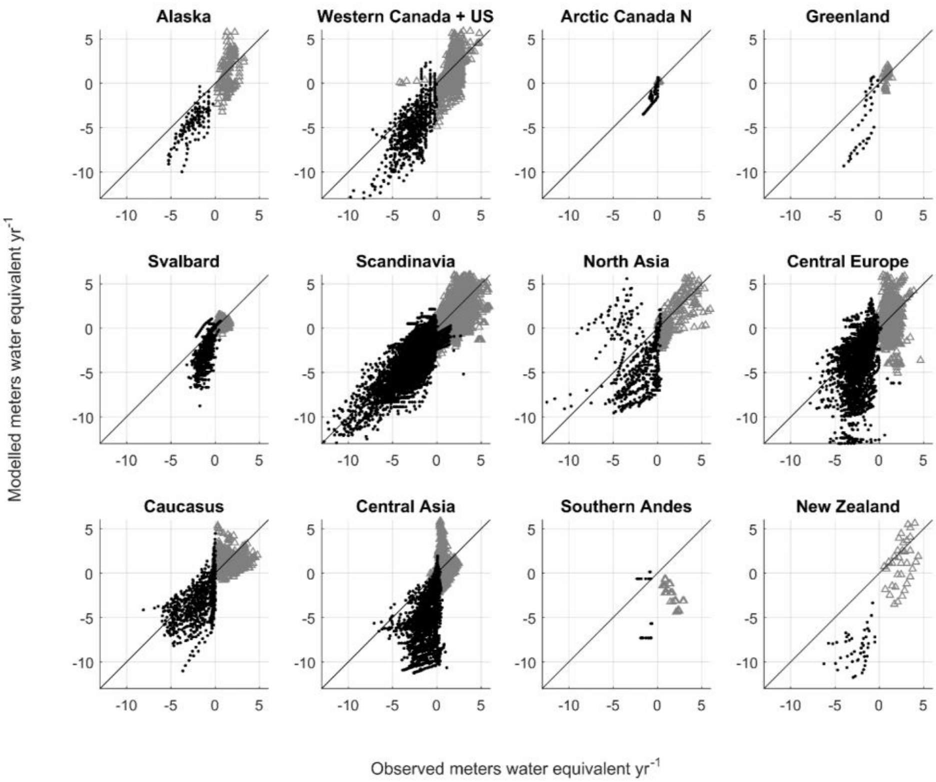

Figure 4~~5~~ Comparison between modelled and observed elevation-band specific mass balance for winter (grey triangles) and summer (black dots). The modelled mass balance is calculated using the tuned regional parameters from the calibration procedure. ~~In the upper left-hand corner is the summer and winter root mean square error and the number of observations in brackets.~~

Table 4 Winter (bold) and summer (italics) number of elevation-band mass balance observations (No obs), root mean square error (RMSE), correlation coefficient (r), Nash–Sutcliffe efficiency coefficient (NS) and mean bias (BIAS).

Region	*No ~~O~~obs*		*RMSE*		*r*		*NS*		*BIAS*	
			m.w.eq.yr^{-1}						*m.w.eq.yr^{-1}*	
Alaska	**127**	127	**1.82**	2.43	**0.38**	0.76	**-7.54**	-2.88	**-0.29**	-2.09
Western Canada and US	**767**	729	**1.76**	2.96	**0.53**	0.72	**-2.68**	-2.25	**-0.34**	-2.28
Arctic Canada North	**49**	50	**0.08**	1.09	**0.09**	0.86	**-0.94**	-5.01	**0.04**	-0.79
Greenland	**28**	36	**0.78**	3.45	**0.33**	0.81	**-11.31**	-11.13	**-0.11**	-2.40
Svalbard	**1,122**	1,126	**0.61**	2.25	**0.18**	0.66	**-3.90**	-12.59	**-0.38**	-1.84
Scandinavia	**5,347**	10,679	**1.52**	1.69	**0.61**	0.78	**-0.78**	0.32	**-0.68**	-0.77
North Asia	**854**	828	**1.54**	4.15	**0.71**	0.20	**-0.40**	-3.81	**-1.08**	-2.63
Central Europe	**5,496**	4,804	**1.21**	2.77	**0.12**	0.33	**-5.83**	-4.63	**-0.02**	-1.11
Caucasus + Middle East	**602**	677	**1.39**	2.30	**-0.12**	0.55	**-1.15**	-0.94	**-0.23**	-1.18
Central Asia	**1,778**	1,751	**1.34**	4.87	**0.21**	0.31	**-10.57**	-16.92	**-0.19**	-4.23
Southern Andes	**34**	22	**4.19**	4.11	**-0.81**	-0.08	**-36.73**	-55.59	**-3.81**	-2.36
New Zealand	**45**	45	**3.37**	6.17	**0.42**	0.32	**-10.63**	-17.82	**-0.01**	-5.87
Global	**16,249**	20,874	**1.38**	2.16	**0.49**	0.78	**-1.16**	0.11	**-0.37**	-0.92

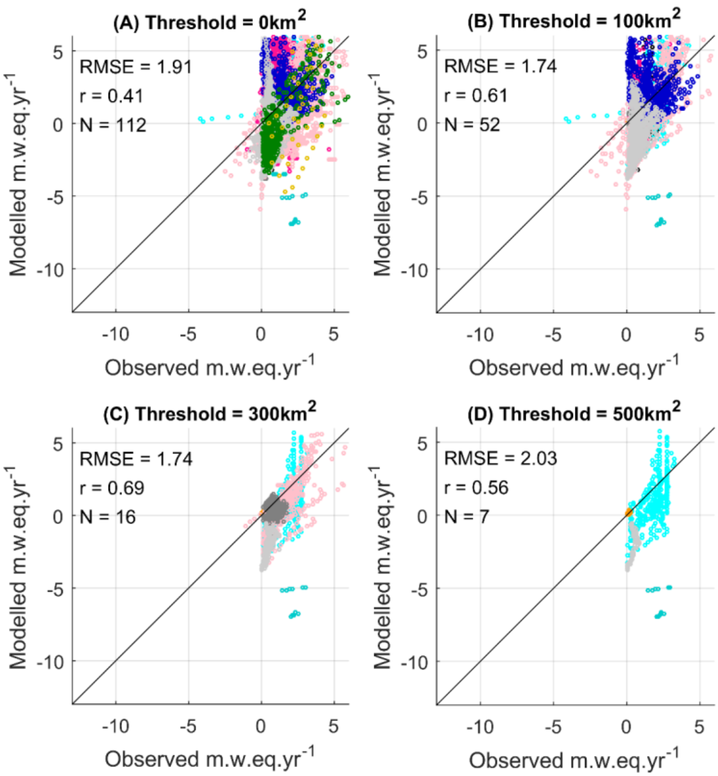

Figure 56 Simulated and observed elevation-dependent winter mass balance when gridboxes with a glacier area of less than 100km², 300km² and 500km² are excluded. The colour identifies the RGI6 regions shown in Figure 2. The RMSE, correlation coefficient and number of glaciers are listed.

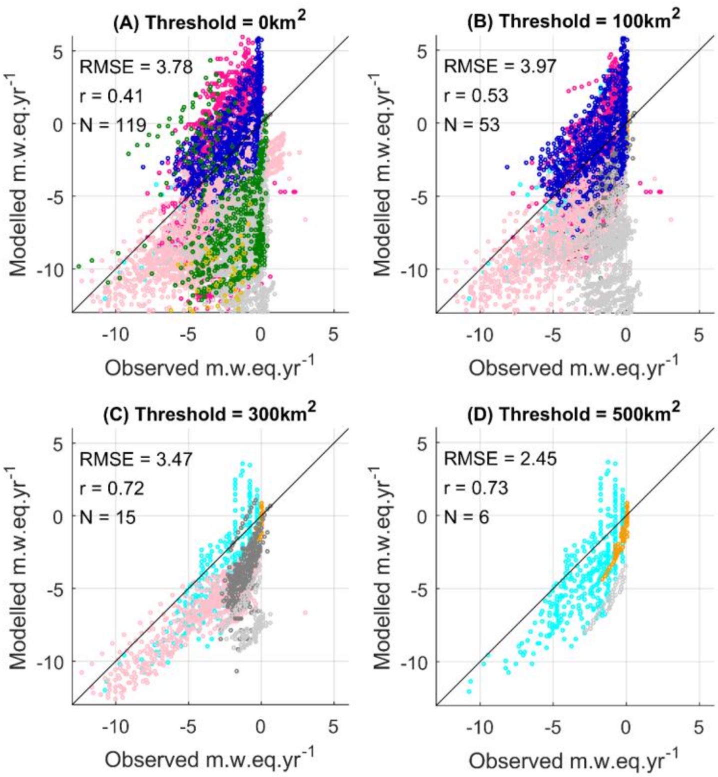

Figure 6~~7~~ Simulated and observed elevation-dependent summer mass balance when gridboxes with a glacier area of less than 100km^2, 300km^2 and 500km^2 are excluded. The colour identifies the RGI6 regions shown in Figure 2. The RMSE, correlation coefficient and number of glaciers are listed.

Table 5 List of high-end climate change CMIP5 models that are downscaled using HadGEM3-A. The years when the CMIP5 models pass +1.5ºC, +2ºC and +4ºC global average warming relative to the pre-industrial period are shown. *No data is available for 2113 because the bias corrected data ends at 2097.

CMIP5 model	*Ensemble member*	*+ 1.5ºC*	*+ 2ºC*	*+ 4ºC*
IPSL-CM5A-LR	r1i1p1	2015	2030	2068
GFDL-ESM2M	r1i1p1	2040	2055	2113*
HadGEM2-ES	r1i1p1	2027	2039	2074
IPSL-CM5A-MR	r1i1p1	2020	2034	2069
MIROC-ESM-CHEM	r1i1p1	2023	2035	2071
HELIX ACCESS1-0	r1i1p1	2034	2046	2085

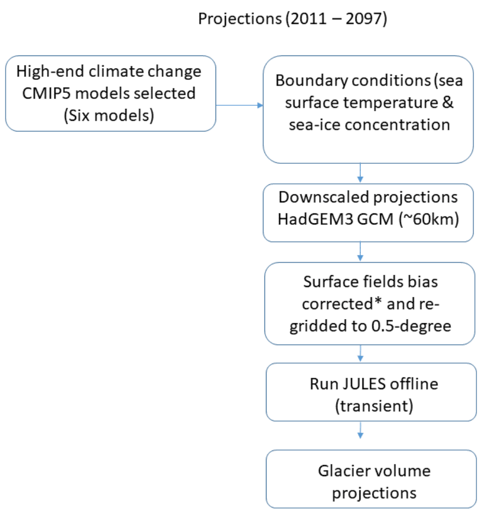

Figure 7~~8~~ Flow chart showing the experimental set up to calculate future glacier volume. *The bias correction method is described by Hempel et al. (2013b)

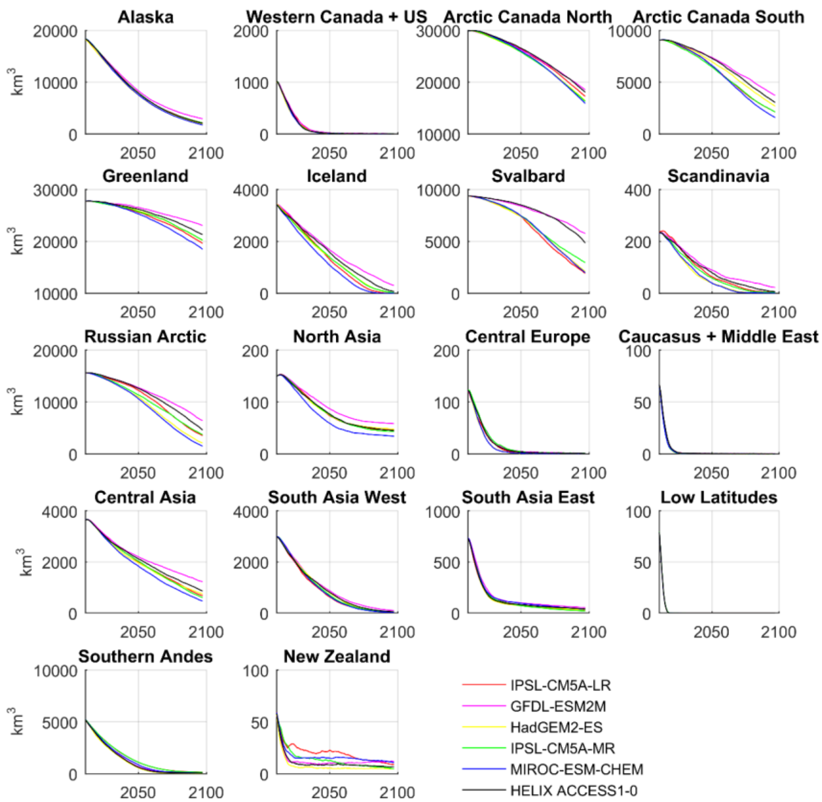

Figure 89 Regional glacier volume projections using the HadGEM3-A ensemble of high-end climate change scenarios.

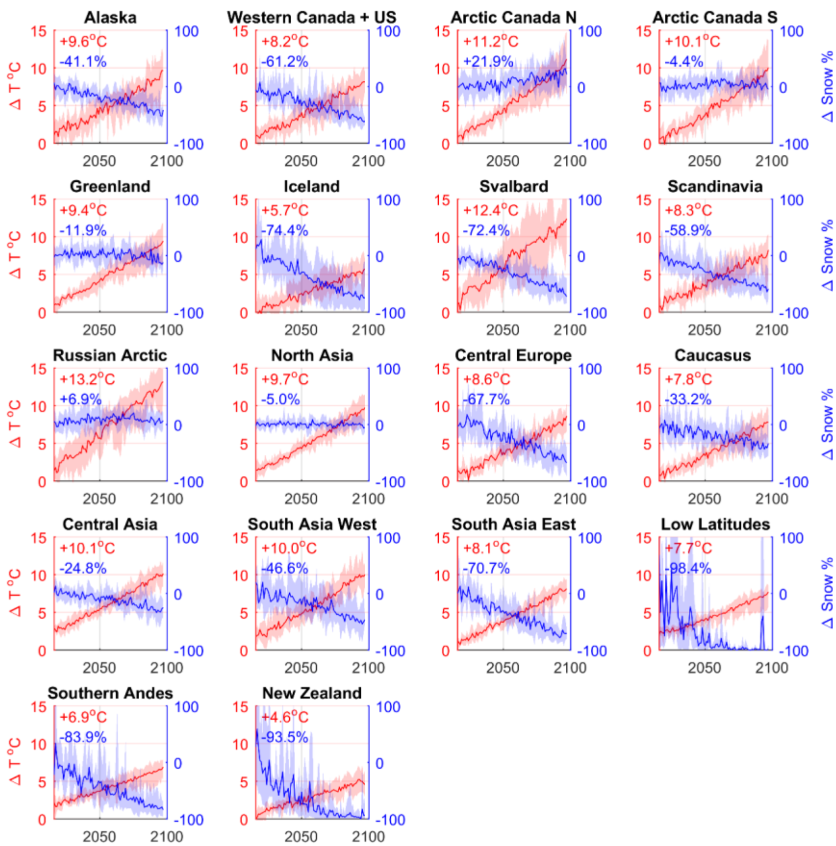

Figure 9~~10~~ Regional temperature and snowfall changes relative to present day (2011-2015) from the HadGEM3-A ensemble over glaciated grid points. The ensemble mean is shown in the solid line and the range of model projections are shown in the shaded regions.

Table 6 Percentage ice volume loss, relative to the initial volume (ΔV) and ice loss in mm of Sea Level Equivalent (SLE) for the end of the century (2097). Percentage volume loses are shown for low, medium and high elevation ranges as well as for all elevations. The data shows the multi-model mean ± one standard deviation. The conversion of volume to SLE assumes an ocean area of 3.618 x 10^8 km^2. The initial area and volume from the Randolph Glacier Inventory Version 6 is listed in columns 1 and 2.

	Area	Volume	ΔV 0m-9000m	ΔV 0m-2000m	ΔV 2250m-4000m	ΔV 4250m-8000m	SLE
	km^2	km^3	%	%	%	%	mmSLE
Alaska	86,616	19,743	-89±2	-93±1	-55±9	408±18	44.6±1.1
Western Canada and US	14,357	1,070	-100±0	-100±0	-99±0	684±136	2.8±0.0
Arctic Canada North	104,920	32,376	-47±3	-43±4	40±1	-	35.8±3.0
Arctic Canada South	40,861	9,780	-74±8	-72±9	-	-	18.1±2.1
Greenland	126,143	29,856	-31±5	-31±6	37±3	-	20.1±4.4
Iceland	11,052	3,722	-98±3	-98±3	-	-	9.3±0.3
Svalbard	33,932	10,112	-68±16	-65±18	608±158	-	17.0±4.6
Scandinavia	2,948	244	-98±3	-97±3	-92±17	-	0.6±0.0
Russian Arctic	51,552	16,908	-79±10	-77±11	-	-	33.3±4.8
North Asia	2,400	156	-71±5	-97±2	-52±8	220±41	0.3±0.0
Central Europe	2,091	127	-99±0	-100±0	-99±0	-77±24	0.3±0.0
Caucasus & Middle East	1,305	71	-100±0	-100±0	-100±0	-99±0	0.2±0.0
Central Asia	48,415	3,849	-80±7	-	-100±0	-74±9	8.0±0.7
South Asia West	29,561	3,180	-98±1	-	-100±0	-98±1	8.1±0.1
South Asia East	11,148	773	-95±2	-	-100±0	-95±2	1.9±0.0
Low Latitudes	2,341	88	-100±0	-100±0	-100±0	-100±0	0.2±0.0
Southern Andes	29,369	5,701	-98±1	-99±1	-74±14	-57±12	14.4±0.1
New Zealand	1,161	65	-88±5	-100±0	71±62	-	0.1±0.0
Global	600,172	137,821	-64±5	-61±6	-36±3	-84±5	215.2±21.3

	~~Area~~	~~Volume~~	~~ΔV~~	~~SLE~~
	~~km^2~~	~~km^3~~	~~2011-2097~~	~~2011-2097~~
~~*Alaska*~~	~~86,616~~	~~19,743~~	~~-89±2~~	~~44.6±1.1~~
~~*Western Canada and US*~~	~~14,357~~	~~1,070~~	~~-100±0~~	~~2.8±0.0~~
~~*Arctic Canada North*~~	~~104,920~~	~~32,376~~	~~-47±3~~	~~35.8±3.0~~
~~*Arctic Canada South*~~	~~40,861~~	~~9,780~~	~~-74±8~~	~~18.1±2.1~~
~~*Greenland*~~	~~126,143~~	~~29,856~~	~~-31±5~~	~~20.1±4.4~~
~~*Iceland*~~	~~11,052~~	~~3,722~~	~~-98±3~~	~~9.3±0.3~~
~~*Svalbard*~~	~~33,932~~	~~10,112~~	~~-68±16~~	~~17.0±4.6~~
~~*Scandinavia*~~	~~2,948~~	~~244~~	~~-98±3~~	~~0.6±0.0~~
~~*Russian Arctic*~~	~~51,552~~	~~16,908~~	~~-79±10~~	~~33.3±4.8~~

~~*North Asia*~~	~~2,400~~	~~156~~	~~-71±5~~	~~0.3±0.0~~
~~*Central Europe*~~	~~2,091~~	~~127~~	~~-99±0~~	~~0.3±0.0~~
~~*Caucasus and Middle East*~~	~~1,305~~	~~71~~	~~-100±0~~	~~0.2±0.0~~
~~*Central Asia*~~	~~48,415~~	~~3,849~~	~~-80±7~~	~~8.0±0.7~~
~~*South Asia West*~~	~~29,561~~	~~3,180~~	~~-98±1~~	~~8.1±0.1~~
~~*South Asia East*~~	~~11,148~~	~~773~~	~~-95±2~~	~~1.9±0.0~~
~~*Low Latitudes*~~	~~2,341~~	~~88~~	~~-100±0~~	~~0.2±0.0~~
~~*Southern Andes*~~	~~29,369~~	~~5,701~~	~~-98±1~~	~~14.4±0.1~~
~~*New Zealand*~~	~~1,161~~	~~65~~	~~-88±5~~	~~0.1±0.0~~
~~*Global*~~	~~600,172~~	~~137,821~~	~~-64±5~~	~~215.2±21.3~~

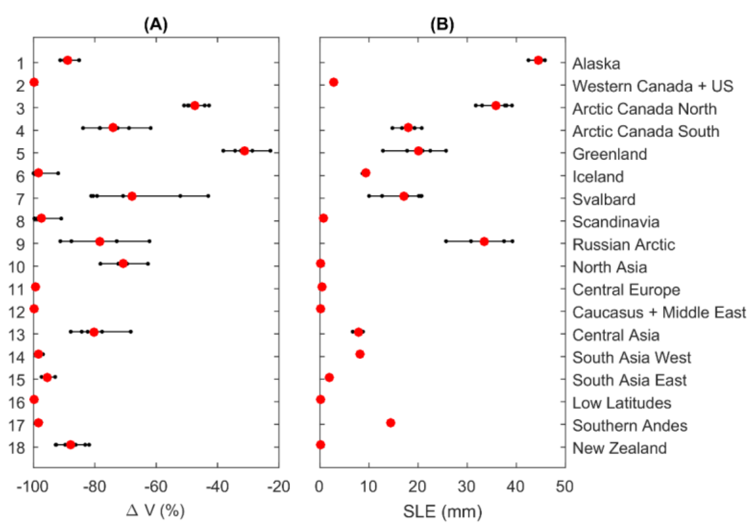

Figure 10~~11~~ (A) Regional percentage volume losses at the end of the century (2097), relative to the initial volume and (B) volume losses expressed in sea-level equivalent contributions. The large red dots represent the multi-model mean and the small black dots are the individual HadGEM3-A model runs.

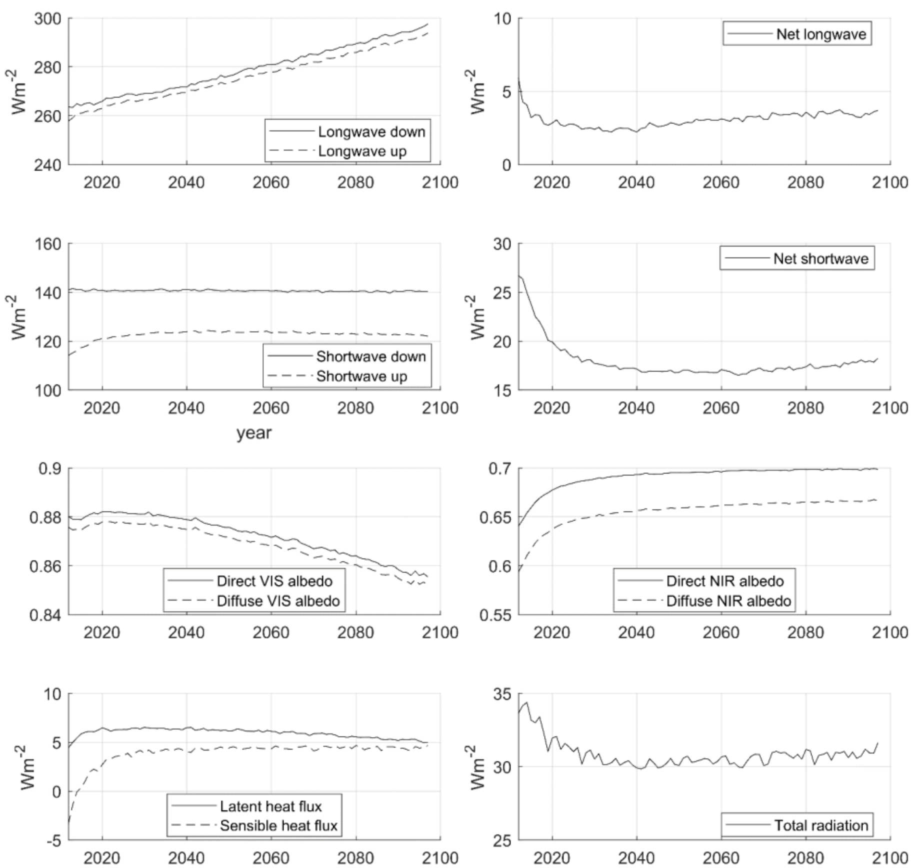

Figure 11 Ensemble mean energy balance components averaged over all glaciated regions and all elevation bands when the model is forced with HadGEM3-A data.

Formatted: Normal

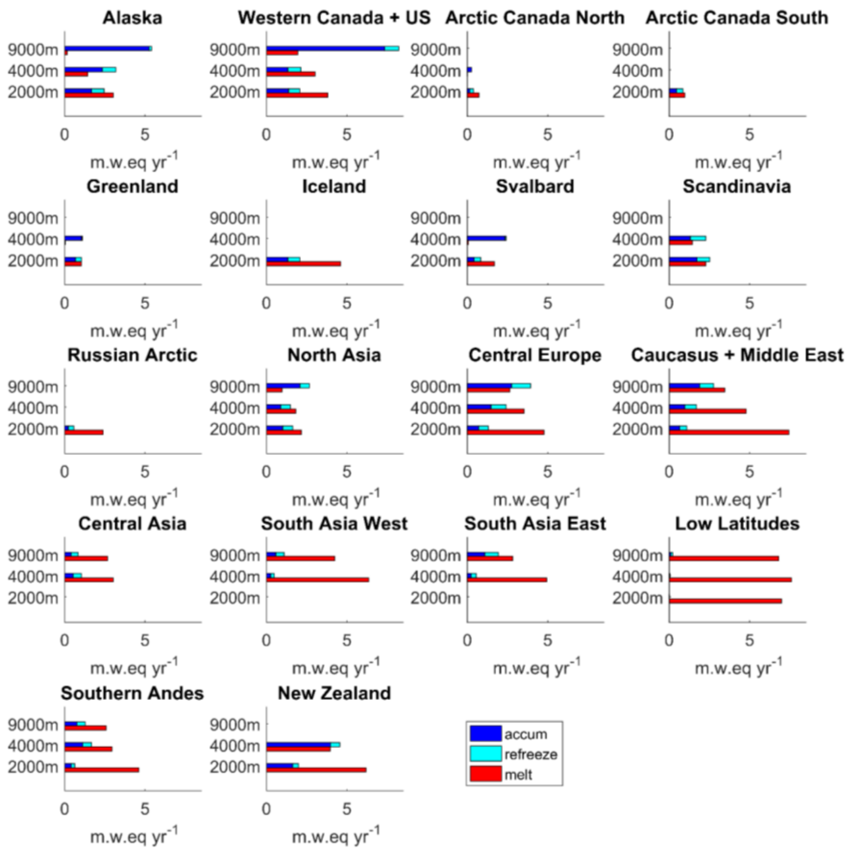

Formatted: Centered, Keep with next

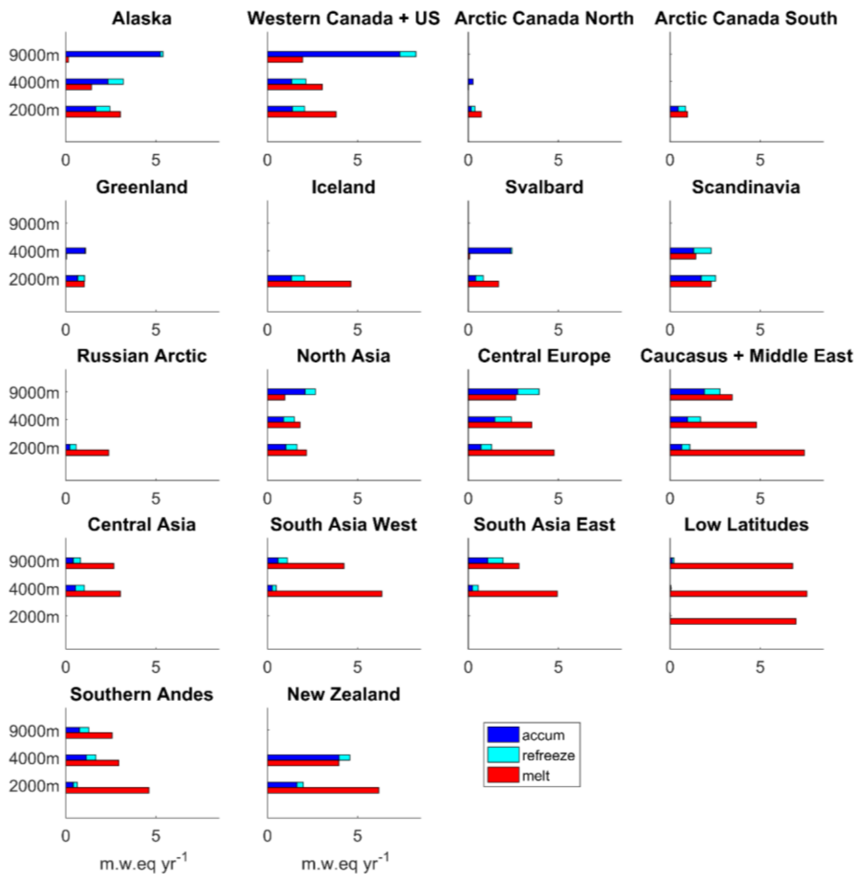

Figure 12~~1212~~ Modelled annual surface mass balance components; accumulation, refreezing and melting for the period 1980-2000 for RGI6 regions. To make the figure easier to read melting is given as positive sign and sublimation is excluded because its contribution is very small. Mass balance components are averaged over low (0-2000m), medium (2250m-4000m) and high (4250-9000m) elevation ranges.

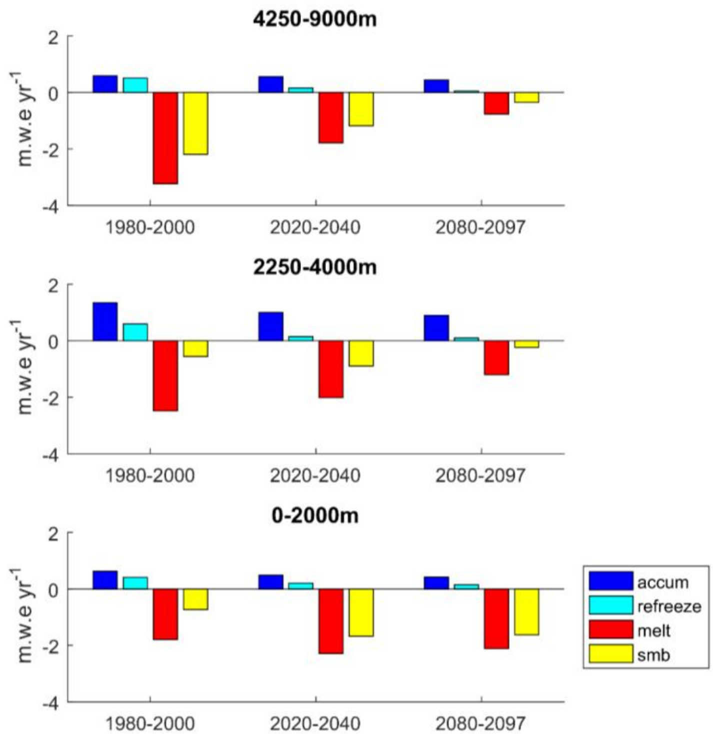

Figure 13~~13~~13 Global mass balance components for three elevation ranges. The historical period is calculated using the WDFEI data and the future period is the multi-model means of all GCMs. The bars show the averages over the time periods for accumulation, refreezing, melt and mass balance rates.

Formatted: Keep with next

Formatted: Caption

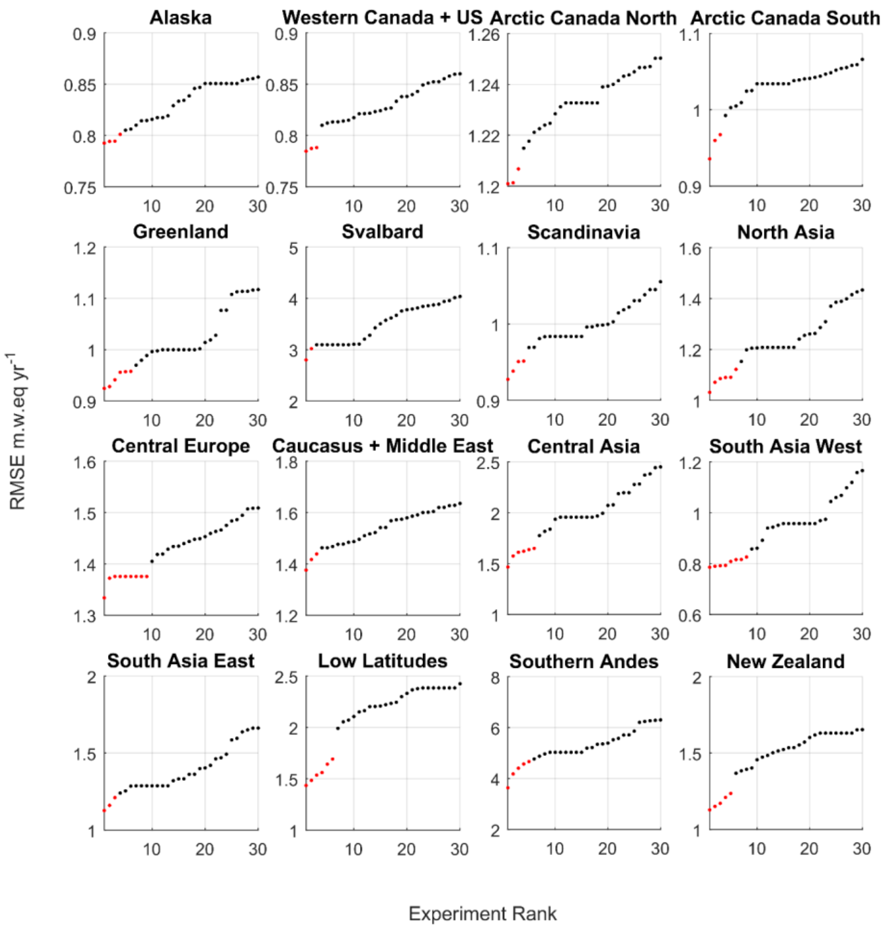

Figure 141414 Calibration experiments raked according the root mean square error between simulated and observed mass balance profiles for RGI6 regions. There are 198 experiments but only the top 30 have been plotted to make the figure easier to read. The red dots indicate experiments that perform equally well.

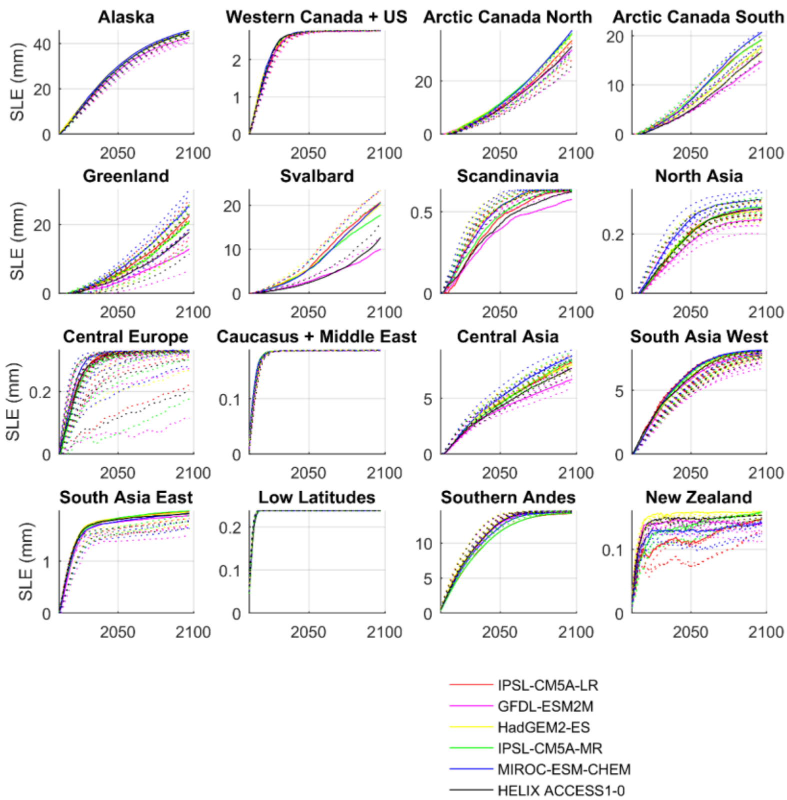

Figure 15~~1515~~ Regional volume losses expressed in sea-level equivalent including parametric uncertainty in mass balance parameters. The solid lines show the volume loss for each downscaled CMIP5 GCM using the optimum parameter sets. The dashed lines are for runs which use other equally 'good' parameter sets based on the RMSE.

Table 7 Regional ensemble mean, minimum and maximum volume losses for 2097 in sea-level equivalent (mm) when the present-day mass balance is calibrated in different ways. Columns 1-3; mass balance is calibrated by minimising the RMSE. Columns 4-6; mass balance is calibrated using an ensemble of equally plausible RMSE values. Columns 7-9; mass balance is calibrated by minimising the RMSE, minimising the bias and maximising the correlation coefficient. ~~when mass balance is cabraring by minimising RMSE, using equally plausible RMSE and using RMSE, Volume losses when calibration parameters are selebed ny minimising the RMSE Min RMSE, (The first three columns using the optimum parameter set for mass balance and the last three columns are for runs which include parametric uncertainty.~~

	Optimum parameter			Equally plausible RMSE			Extra performance metrics		
	SLE_{mean}	SLE_{min}	SLE_{max}	SLE_{mean}	SLE_{min}	SLE_{max}	SLE_{mean}	SLE_{min}	SLE_{max}
Alaska	44.6	42.5	45.8	43.8	40.5	45.8	43.6	38.2	46.3
Western Canada and US	2.8	2.8	2.8	2.8	2.8	2.8	2.8	2.8	2.8
Arctic Canada North	35.8	31.8	39.1	32.8	24.3	39.1	37.2	22.3	61.8
Arctic Canada South	18.1	14.8	20.8	17.9	13.7	21.1	20.3	14.8	24.1
Greenland	20.1	12.9	25.7	20.4	6.7	30.2	23.5	14.0	31.8
Iceland	9.3	8.7	9.5	9.3	8.7	9.5	9.4	8.5	9.5
Svalbard	17.0	10.0	20.7	18.4	10.0	23.6	19.7	10.0	25.8
Scandinavia	0.6	0.6	0.6	0.6	0.6	0.6	0.6	0.6	0.6
Russian Arctic	33.3	25.7	39.2	33.3	25.7	39.2	36.6	25.1	42.8
North Asia	0.3	0.3	0.3	0.3	0.2	0.4	0.3	0.3	0.4
Central Europe	0.3	0.3	0.3	0.3	0.1	0.3	0.3	0.2	0.3
Caucasus and Middle East	0.2	0.2	0.2	0.2	0.2	0.2	0.2	0.2	0.2
Central Asia	8.0	6.7	8.8	8.0	5.9	9.3	8.1	5.9	9.5
South Asia West	8.1	8.0	8.2	7.8	6.7	8.2	7.9	7.1	8.2
South Asia East	1.9	1.9	2.0	1.8	1.5	2.0	1.8	1.6	2.0
Low Latitudes	0.2	0.2	0.2	0.2	0.2	0.2	0.2	0.2	0.2
Southern Andes	14.4	14.2	14.5	14.4	14.2	14.6	14.4	14.2	14.6
New Zealand	0.1	0.1	0.2	0.1	0.1	0.2	0.1	0.1	0.2
Global	215.2	181.5	238.9	212.6	162.2	247.3	227.1	166.1	281.1
Global SLE_{max} - SLE_{min}	57.3			85.1			115.0		

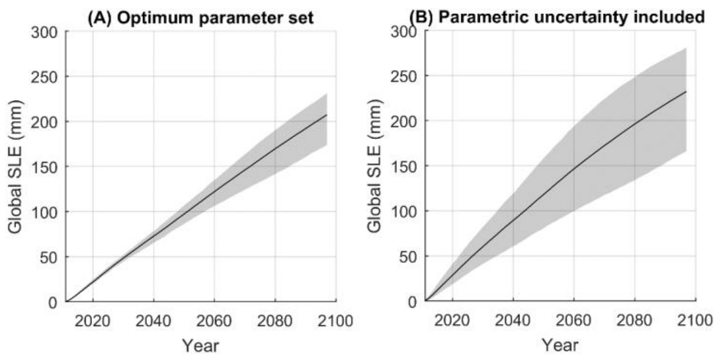

Figure 16~~16~~16 Multi-model mean (black line) and ensemble spread (shaded) global volume loss in sea-level equivalent. (A) is the volume loss when optimum parameters sets are selected by minimising the RMSE and (B) is volume loss when optimum parameters sets are selected using additional performance metrics (minimising RMSE, minimising the bias and maximising the correlation coefficient).

Code Availability

The glacier scheme is included in JULES v4.7. The source code can be downloaded by accessing the Met Office Science Repository Service (MOSRS) (requires registration): https://code.metoffice.gov.uk/ The code used for this study is in https://code.metoffice.gov.uk/svn/jules/main/branches/dev/sarahshannon/vn4.7_va_scaling

Formatted: Normal

Formatted: Normal

Acknowledgements

Thise research ~~leading to these results~~ was funded by ~~from t~~the European Union Seventh Framework Programme FP7/2007-2013 under grant agreement n° 603864. We would like to thank the Natural Environment Research Council (NERC) for the use of the ~~-~~Joint Analysis System Meeting Infrastructure Needs (JASMIN) super computer cluster.

Formatted: Font: Times New Roman, 10 pt, Font color: Auto, Pattern: Clear

References

Ageta, Y., and Higuchi, K.: Estimation of mass balance components of a summer-accumulation type glacier in the Nepal Himalaya, Geografiska Annaler Series a-Physical Geography, 66, 249-255, 10.2307/520698, 1984.

Bahr, D. B., Meier, M. F., and Peckham, S. D.: The physical basis of glacier volume-area scaling, Journal of Geophysical Research-Solid Earth, 102, 20355-20362, 10.1029/97jb01696, 1997.

Bell, V. A., Kay, A. L., Jones, R. G., and Moore, R. J.: Development of a high resolution grid-based river flow model for use with regional climate model output, Hydrology and Earth System Sciences, 11, 532-549, 2007.

Benn, D. I., Kirkbride, M., Owen, L. A., and Brazier, V.: Glaciated Valley Landsystems, Hodder Education, Glacial landsystems, D.J.A. Evans (Ed.), London, 372-406 pp., 2005.

Best, M. J., Pryor, M., Clark, D. B., Rooney, G. G., Essery, R. L. H., Ménard, C. B., Edwards, J. M., Hendry, M. A., Porson, A., Gedney, N., Mercado, L. M., Sitch, S., Blyth, E., Boucher, O., Cox, P. M., Grimmond, C. S. B., and Harding, R. J.: The Joint UK Land Environment Simulator (JULES), model description – Part 1: Energy and water fluxes, Geosci. Model Dev., 4, 677-699, 10.5194/gmd-4-677-2011, 2011.

Bliss, A., Hock, R., and Radic, V.: Global response of glacier runoff to twenty-first century climate change, Journal of Geophysical Research-Earth Surface, 119, 717-730, 10.1002/2013jf002931, 2014.

Bosson, J. B., and Lambiel, C.: Internal Structure and Current Evolution of Very Small Debris-Covered Glacier Systems Located in Alpine Permafrost Environments, Frontiers in Earth Science, 4, 10.3389/feart.2016.00039, 2016.

Bruland, O., and Hagen, J. O.: Glacial mass balance of Austre Broggerbreen (Spitsbergen), 1971-1999, modelled with a precipitation-run-off model, Polar Research, 21, 109-121, 10.1111/j.1751-8369.2002.tb00070.x, 2002.

Chen, X. L., and Zhou, T. J.: Distinct effects of global mean warming and regional sea surface warming pattern on projected uncertainty in the South Asian summer monsoon, Geophysical Research Letters, 42, 9433-9439, 10.1002/2015gl066384, 2015.

Farinotti, D., Huss, M., Bauder, A., Funk, M., and Truffer, M.: A method to estimate the ice volume and ice-thickness distribution of alpine glaciers, Journal of Glaciology, 55, 422-430, 10.3189/002214309788816759, 2009.

Gardner, A. S., Moholdt, G., Cogley, J. G., Wouters, B., Arendt, A., A.Wahr, J., Berthier, E., Hock, R., Pfeffer, W. T., Kaser, G., Ligtenberg, S. R. M., Bolch, T., Sharp, M. J., Hagen, J. O., van den Broeke, M. R., and Paul, F.: A Reconciled Estimate of Glacier Contributions to Sea Level Rise: 2003 to 2009, Science, 340, 852-857, 10.1126/science.1234532, 2013.

Giesen, R. H., and Oerlemans, J.: Climate-model induced differences in the 21st century global and regional glacier contributions to sea-level rise, Climate Dynamics, 41, 3283-3300, 10.1007/s00382-013-1743-7, 2013.

Gohar, L. K., Lowe, J. A., and Bernie, D.: The Impact of Bias Correction and Model Selection on Passing Temperature Thresholds, Journal of Geophysical Research-Atmospheres, 122, 12045-12061, 10.1002/2017jd026797, 2017.

Greuell, W., and Konzelmann, T.: Numerical modelling of the energy balance and the englacial temperature of the Greenland Ice Sheet, Calculations for the ETH Camp location (West Greenland, 1155 m a.s.l.), Global and Planetary Change, 9, 91-114, 10.1016/0921-8181(94)90010-8, 1994.

Greuell, W., and Smeets, P.: Variations with elevation in the surface energy balance on the Pasterze (Austria), Journal of Geophysical Research-Atmospheres, 106, 31717-31727, 10.1029/2001jd900127, 2001.

Hadley, O. L., and Kirchstetter, T. W.: Black-carbon reduction of snow albedo, Nature Climate Change, 2, 437-440, 10.1038/nclimate1433, 2012.

Hempel, S., Frieler, K., Warszawski, L., Schewe, J., and Piontek, F.: A trend-preserving bias correction – the ISI-MIP approach, Earth System Dynamics, 4, 219-236, 10.5194/esd-4-219-2013, 2013.

Hirabayashi, Y., Doll, P., and Kanae, S.: Global-scale modeling of glacier mass balances for water resources assessments: Glacier mass changes between 1948 and 2006, Journal of Hydrology, 390, 245-256, 10.1016/j.jhydrol.2010.07.001, 2010.

Hirabayashi, Y., Zang, Y., Watanabe, S., Koirala, S., and Kanae, S.: Projection of glacier mass changes under a high-emission climate scenario using the global glacier model HYOGA2, Hydrological Research Letters, 7, 6-11, 10.3178/HRL.7.6, 2013.

Hock, R.: Glacier melt: a review of processes and their modelling, Progress in Physical Geography, 29, 362-391, 10.1191/0309133305pp453ra, 2005.

Hudson, S. R., Warren, S. G., Brandt, R. E., Grenfell, T. C., and Six, D.: Spectral bidirectional reflectance of Antarctic snow: Measurements and parameterization, Journal of Geophysical Research-Atmospheres, 111, 10.1029/2006jd007290, 2006.

Huss, M., Funk, M., and Ohmura, A.: Strong Alpine glacier melt in the 1940s due to enhanced solar radiation, Geophysical Research Letters, 36, L23501, 10.1029/2009gl040789, 2009.

Huss, M., and Farinotti, D.: Distributed ice thickness and volume of all glaciers around the globe, Journal of Geophysical Research, 117, F04010, 10.1029/2012JF002523, 2012.

Huss, M., and Hock, R.: A new model for global glacier change and sea-level rise, Frontiers in Earth Science, 3, 54, 10.3389/feart.2075.00054, 2015.

Huss, M., and Hock, R.: Global-scale hydrological response to future glacier mass loss, Nature Climate Change, 8, 135-140, 10.1038/s41558-017-0049-x, 2018.

Immerzeel, W. W. P., F. Bierkens, M. F. P.: Rising river flows throughout the twenty-first century in two Himalayan glacierized watersheds, Nature Geoscience, 3, 742–745 10.1038/ngeo1896, 2013.

Kaser, G., Cogley, J. G., Dyurgerov, M. B., Meier, M. F., and Ohmura, A.: Mass balance of glaciers and ice caps: Consensus estimates for 1961-2004, Geophysical Research Letters, 33, 10.1029/2006gl027511, 2006.

Kotlarski, S., Jacob, D., Podzun, R., and Paul, F.: Representing glaciers in a regional climate model, Climate Dynamics, 34, 27-46, 10.1007/s00382-009-0685-6, 2010.

Lambrecht, A., Mayer, C., Hagg, W., Popovnin, V., Rezepkin, A., Lomidze, N., and Svanadze, D.: A comparison of glacier melt on debris-covered glaciers in the northern and southern Caucasus, Cryosphere, 5, 525-538, 10.5194/tc-5-525-2011, 2011.

Landolt-Bornstein: Numerical Data and Functional Relationships in Science and Technology, Group V Geophysics and Space Research, Physical and Chemical Properties of Air, p 35, 4B Meteorology, 1987.

Lardeux, P., Glasser, N., Holt, T., and Hubbard, B.: Glaciological and geomorphological map of Glacier Noir and Glacier Blanc, French Alps, Journal of Maps, 12, 582-596, 10.1080/17445647.2015.1054905, 2016.

Lavielle, M.: Using penalized contrasts for the change-point problem., Signal Processing, 85, 1501–1510, 2005.

Lutz, A. F., Immerzeel, W. W., Shrestha, A. B., and Bierkens, M. F. P.: Consistent increase in High Asia's runoff due to increasing glacier melt and precipitation, Nature Climate Change, 4, 587–592, 10.1038/nclimate2237, 2014.

Marshall, S. J., and Clarke, G. K. C.: Ice sheet inception: subgrid hypsometric parameterization of mass balance in an ice sheet model (vol 15, pg 533, 1999), Climate Dynamics, 16, 319-319, 2000.

Marzeion, B., Jarosch, A. H., and Hofer, M.: Past and future sea-level change from the surface mass balance of glaciers, The Cryosphere Discuss., 6, 3177-3241, 10.5194/tcd-6-3177-2012, 2012.

McKay, M. D., Beckman, R. J., and Conover, W. J.: Comparison of Three Methods for Selecting Values of Input Variables in the Analysis of Output from a Computer Code, Technometrics, 21, 239-245, 1979.

Meier, M. F., Dyurgerov, M. B., Rick, U. K., O'Neel, S., Pfeffer, W. T., Anderson, R. S., Anderson, S. P., and Glazovsky, A. F.: Glaciers Dominate Eustatic Sea-Level Rise in the 21st Century, Science, 317, 1064-1067, 10.1126/science.1143906, 2007.

Monnier, S., and Kinnard, C.: Pluri-decadal (1955-2014) evolution of glacier-rock glacier transitional landforms in the central Andes of Chile (30-33 degrees S), Earth Surface Dynamics, 5, 493-509, 10.5194/esurf-5-493-2017, 2017.

Oerlemans, J., and Grisogono, B.: Glacier winds and parameterisation of the related surface heat fluxes, Tellus Series a-Dynamic Meteorology and Oceanography, 54, 440-452, 10.1034/j.1600-0870.2002.201398.x, 2002.

Oki, T., T. Nishimura, and P. A. Dirmeyer: Assessment of annual runoff from land surface models using Total Runoff Integrating Pathways (TRIP), Journal of the Meteorological Society of Japan, 77, 135–255, 1999.

Osborne, T. G., J. Hooker, J. Williams, K. Wiltshire, A. Betts, R. Wheeler, T.: JULES-crop: a parametrisation of crops in the Joint UK Land Environment Simulator, Geosci. Model Dev. Discuss., 7, 10.5194/gmdd-7-6773-2014, 2014.

Pellicciotti, F., Carenzo, M., Bordoy, R., and Stoffel, M.: Changes in glaciers in the Swiss Alps and impact on basin hydrology: Current state of the art and future research, Science of the Total Environment, 493, 1152-1170, 10.1016/j.scitotenv.2014.04.022, 2014.

Radić, V., and Hock, R.: Regionally differentiated contribution of mountain glaciers and ice caps to future sea-level rise, Nature Geoscience, 4, 91-94, 10.1038/ngeo1052, 2011.

Radić, V., Bliss, A., Beedlow, A. C., Hock, R., Miles, E., and Cogley, J. G.: Regional and global projections of twenty-first century glacier mass changes in response to climate scenarios from global climate models, Climate Dynamics, 42, 37-58, 10.1007/s00382-013-1719-7, 2014.

Raftery, A. E., Zimmer, A., Frierson, D. M. W., Startz, R., and Liu, P. R.: Less than 2 degrees C warming by 2100 unlikely, Nature Climate Change, 7, 637, 10.1038/nclimate3352, 2017.

Rangecroft, S., Suggitt, A. J., Anderson, K., and Harrison, S.: Future climate warming and changes to mountain permafrost in the Bolivian Andes, Climatic Change, 137, 231-243, 10.1007/s10584-016-1655-8, 2016.

Rasmussen, R., Baker, B., Kochendorfer, J., Meyers, T., Landolt, S., Fischer, A. P., Black, J., Theriault, J. M., Kucera, P., Gochis, D., Smith, C., Nitu, R., Hall, M., Ikeda, K., and Gutmann, E.: How well are we measusing snow? The NOAA/FAA/NCAR Winter Precipitation Test Bed, Bulletin of the American Meteorological Society, 93, 811-829, 10.1175/bams-d-11-00052.1, 2012.

Rebecca, K., Fearnhead, P., and Eckley, I. A.: Optimal detection of changepoints with a linear computational cost, Journal of the American Statistical Association, 107, 1590–1598, 2012.

Reijmer, C. H., Bintanja, R., and Greuell, W.: Surface albedo measurements over snow and blue ice in thematic mapper bands 2 and 4 in Dronning Maud Land, Antarctica, Journal of Geophysical Research-Atmospheres, 106, 9661-9672, 10.1029/2000jd900718, 2001.

RGI Consortium: Randolph Glacier Inventory – A Dataset of Global Glacier Outlines: Version 6.0, Colorado, USA, Digital Media., 2017.

Roesch, A., Wild, M., Pinker, R., and Ohmura, A.: Comparison of spectral surface albedos and their impact on the general circulation model simulated surface climate, Journal of Geophysical Research-Atmospheres, 107, 10.1029/2001jd000809, 2002.

Rogelj, J., den Elzen, M., Hohne, N., Fransen, T., Fekete, H., Winkler, H., Chaeffer, R. S., Ha, F., Riahi, K., and Meinshausen, M.: Paris Agreement climate proposals need a boost to keep warming well below 2 degrees C, Nature, 534, 631-639, 10.1038/nature18307, 2016.

Singh, P.: Snow and Glacier Hydrology, 1 ed., Water Science and Technology Library, Springer Netherlands, 2001.

Slangen, A. B. A., Carson, M., Katsman, C. A., van de Wal, R. S. W., Kohl, A., Vermeersen, L. L. A., and Stammer, D.: Projecting twenty-first century regional sea-level changes, Climatic Change, 124, 317-332, 10.1007/s10584-014-1080-9, 2014.

Sorg, A., Bolch, T., Stoffel, M., Solomina, O., and Beniston, M.: Climate change impacts on glaciers and runoff in Tien Shan (Central Asia), Nature Climate Change, 2, 725-731, 10.1038/nclimate1592, 2012.

Sorg, A., Huss, M., Rohrer, M., and Stoffel, M.: The days of plenty might soon be over in glacierized Central Asian catchments, Environmental Research Letters, 9, doi:10.1088/1748-9326/9/10/104018, 2014.

Stone, E. J., Lunt, D. J., Rutt, I. C., and Hanna, E.: Investigating the sensitivity of numerical model simulations of the modern state of the Greenland ice-sheet and its future response to climate change, Cryosphere, 4, 397-417, 10.5194/tc-4-397-2010, 2010.

Walters, D., Boutle, I., Brooks, M., Melvin, T., Stratton, R., Vosper, S., Wells, H., Williams, K., NigelWood, Allen, T., Bushell, A., Copsey, D., Earnshaw, P., Edwards, J., Gross, M., Hardiman, S., Harris, C., Heming, J., Klingaman, N., Levine, R., Manners, J., Martin, G., Milton, S., Mittermaier, M., Morcrette, C., Riddick, T., Roberts, M., Sanchez, C., Selwood, P., Stirling, A., Smith, C., Suri, D., Tennant, W., Vidale, P. L., JonathanWilkinson, Willett, M., Woolnough, S., and Xavier, P.: The Met Office Unified Model Global Atmosphere 6.0/6.1 and JULES Global Land 6.0/6.1 configurations, Geoscientific Model Development, 10, 1487-1520, 10.5194/gmd-10-1487-2017, 2017.

Warren, S. G., and Wiscombe, W. J.: A model for the spectral albedo of snow, 1. Pure snow, Journal of Atmospheric Science, 37, 2712-2733, 1980.

Weedon, G. P., Gomes, S., Viterbo, P., Shuttleworth, W. J., Blyth, E., Osterle, H., Adam, J. C., Bellouin, N., Boucher, O., and Best, M.: Creation of the WATCH Forcing Data and Its Use to Assess Global and Regional Reference Crop Evaporation over Land during the Twentieth Century, Journal of Hydrometeorology, 12, 823-848, 10.1175/2011jhm1369.1, 2011.

Weedon, G. P., Balsamo, G., Bellouin, N., Gomes, S., J., M., and Viterbo, P.: The WFDEI meteorological forcing data set: WATCH Forcing Data methodology applied to ERA-Interim reanalysis data, Water Resources Research, 10.1002/2014WR015638, 2014.

WGMS, Zemp, M., Nussbaumer, S. U., Gärtner-Roer, I., Huber, J., Machguth, H., Paul, F., and Hoelzle, M.: Global Glacier Change Bulletin No. 2 (2014-2015), World Glacier Monitoring Service, 10.5904/wgms-fog-2017-10, 2017.

Zhang, Y. L., Kang, S. C., Cong, Z. Y., Schmale, J., Sprenger, M., Li, C. L., Yang, W., Gao, T. G., Sillanpaa, M., Li, X. F., Liu, Y. J., Chen, P. F., and Zhang, X. L.: Light-absorbing impurities enhance glacier albedo reduction in the southeastern Tibetan plateau, Journal of Geophysical Research-Atmospheres, 122, 6915-6933, 10.1002/2016jd026397, 2017.

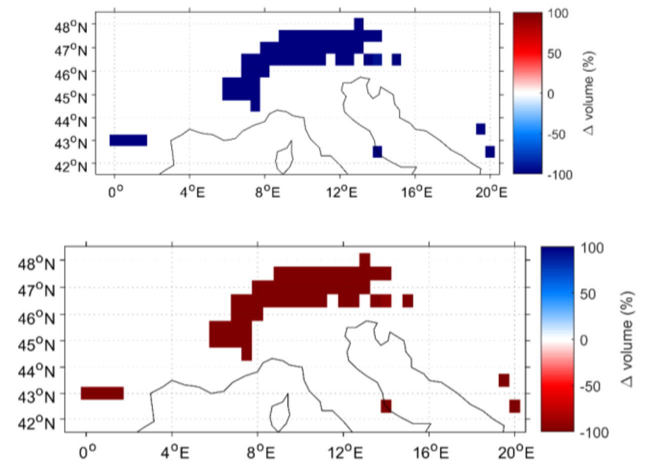

Figure S1 Percentage volume change at 2097, relative to the initial volume for Central Europe.

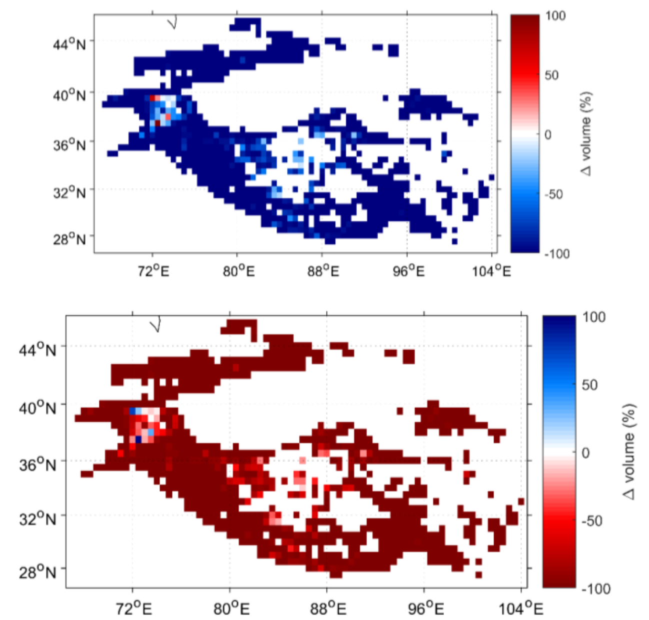

Figure S2 Percentage volume change at 2097, relative to the initial volume for Central Asia, East and West Asia.

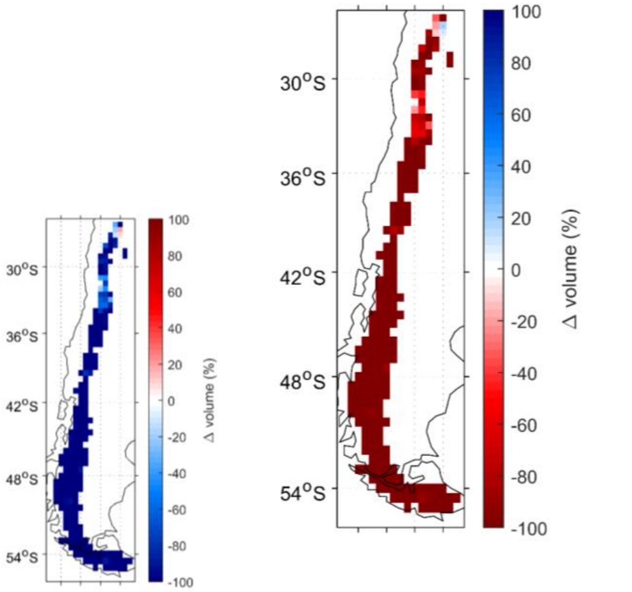

Figure S3 Percentage volume change at 2097, relative to the initial volume for the Southern Andes.

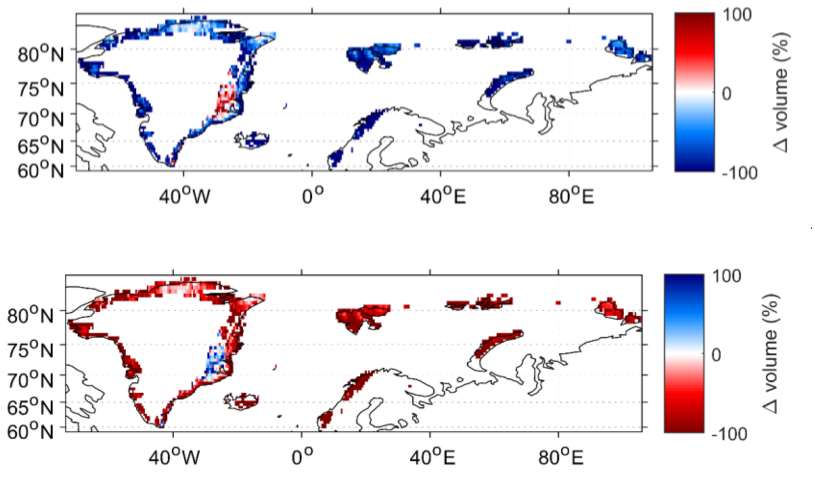

Figure S4 Percentage volume change at 2097, relative to the initial volume for Greenland, Iceland, Svalbard, Scandinavia and the Russian Arctic.

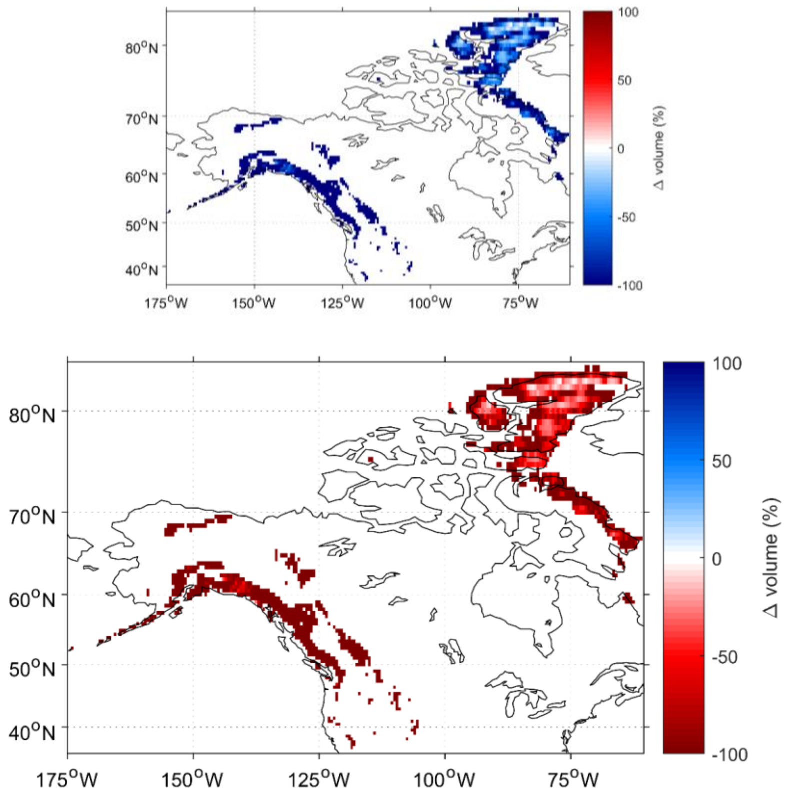

Figure S5 Percentage volume change at 2097, relative to the initial volume for Alaska, Western Canada + US, Arctic Canada North and South.

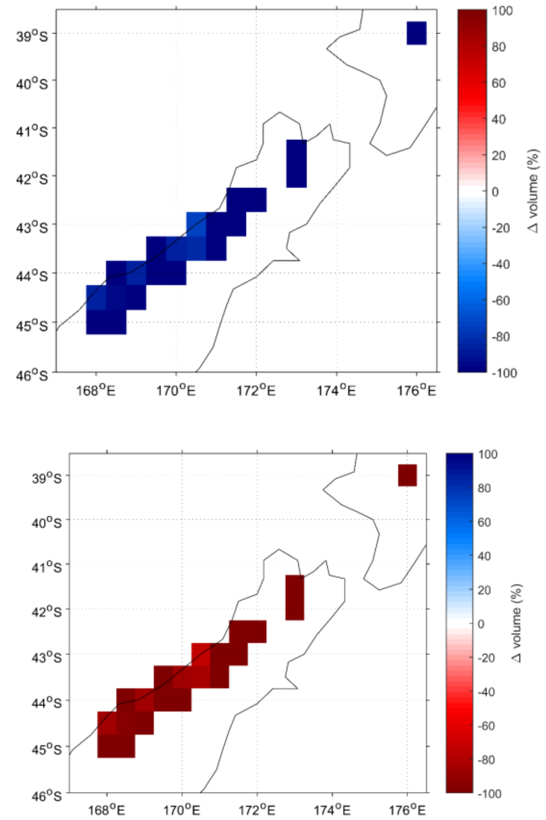

Figure S6 Percentage volume change at 2097, relative to the initial volume for New Zealand.

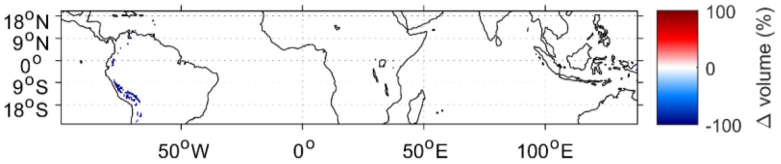

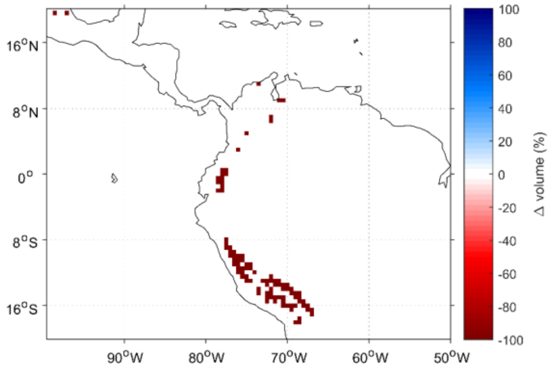

Figure S7 Percentage volume change at 2097, relative to the initial volume for south and Central America~~the Low Latitudes~~

Formatted: Don't keep with next

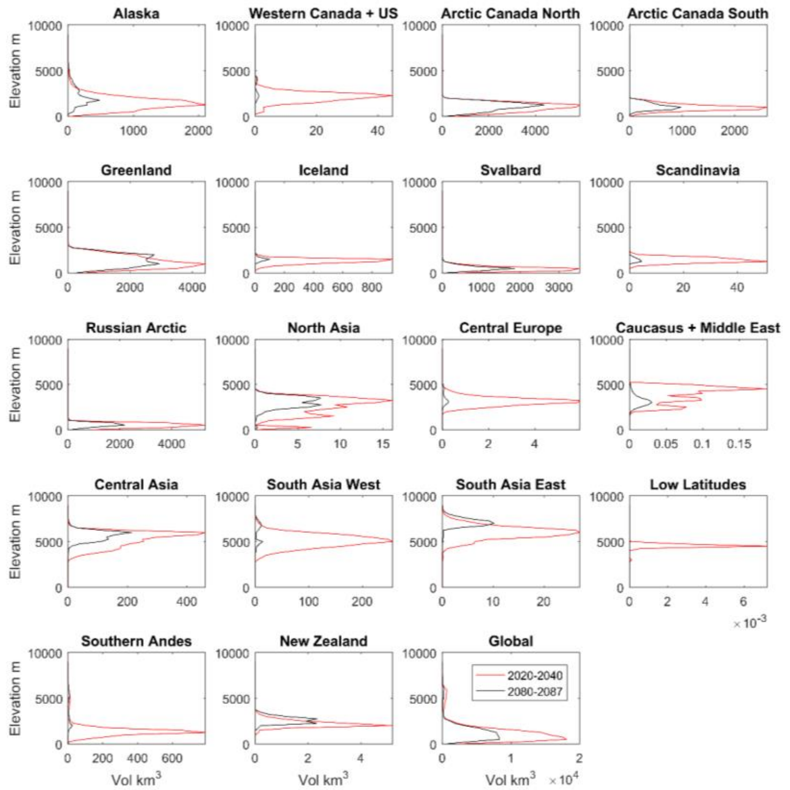

Figure S8 Cumulative mass balances as a function of height for the middle (2020-2040) and end of the century (2080-2087). The projections are the mean of the HadGEM3-A ensemble.

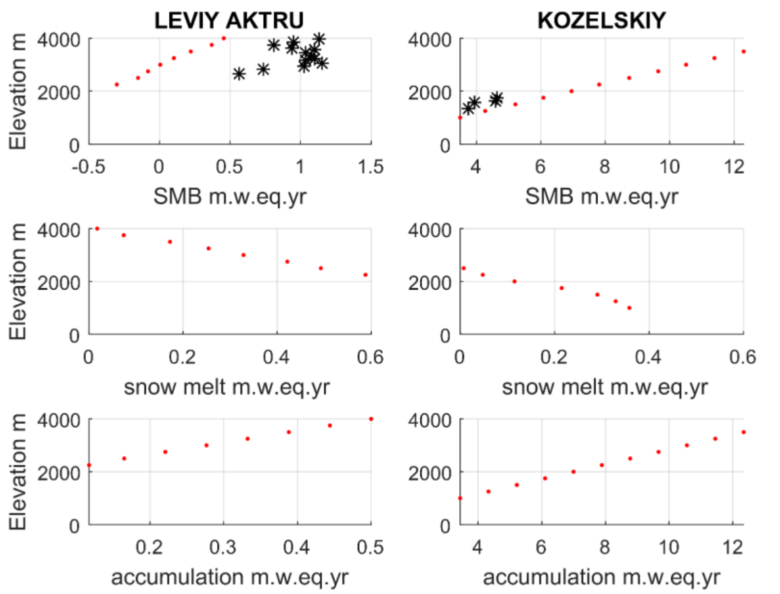

Figure S9 Simulated winter mass balance, snow melt and accumulation for the year 1989 when the model is forced with WFDEI data. The black stars are the elevation-dependant specific mass balance observations.

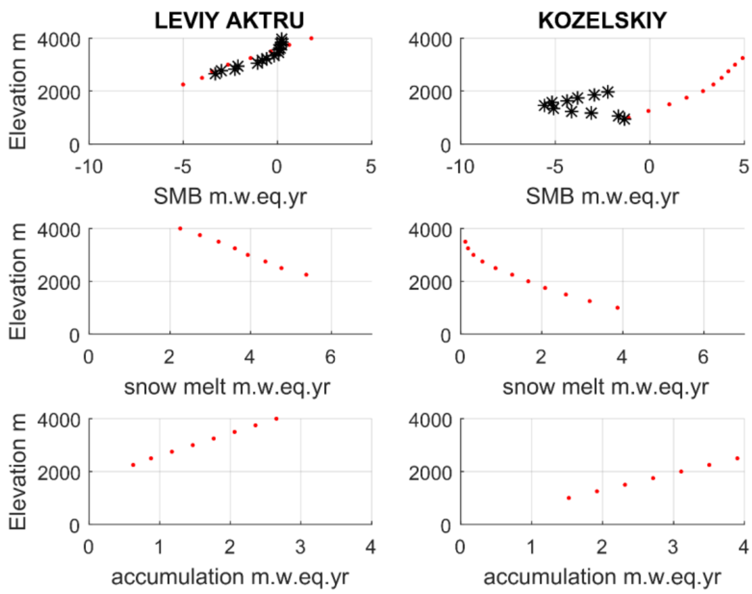

Figure S10 Simulated summer mass balance, snow melt and accumulation for the year 1992 when the model is forced with WFDEI data. The black stars are the elevation-dependant specific mass balance observations.

Table S1 Equally plausible parameter sets derived from the root mean square error for each RGI6 region. Best parameter sets are shown in bold.

	$\alpha_{vis,snow}$	$\alpha_{nir,snow}$	$\alpha_{vis,ice}$	$\alpha_{nir,ice}$	γ_{temp} (°K km^{-1})	γ_{precip} (%/100m)	γ_{wind}
Alaska	**0.88**	**0.65**	**0.56**	**0.27**	**8.16**	**16.46**	**1.32**
	0.95	0.72	0.41	0.19	7.96	14.71	1.07
	0.96	0.76	0.48	0.24	9.11	11.10	1.28
	0.93	0.71	0.65	0.23	7.83	7.80	1.08
Western Canada and US	**0.97**	**0.64**	**0.45**	**0.26**	**9.35**	**7.87**	**2.29**
	0.99	0.79	0.32	0.16	7.67	7.11	2.19
	0.89	0.67	0.49	0.37	8.44	8.22	1.87
Arctic Canada North	**0.96**	**0.70**	**0.49**	**0.12**	**4.22**	**7.35**	**1.10**
	0.98	0.68	0.53	0.23	6.53	6.91	1.46
	0.93	0.71	0.65	0.23	7.83	7.80	1.08
Arctic Canada South	**0.94**	**0.77**	**0.68**	**0.53**	**8.30**	**16.34**	**2.15**
	0.89	0.67	0.49	0.37	8.44	8.22	1.87
	0.91	0.73	0.67	0.56	5.32	8.57	1.55
Greenland	**0.95**	**0.72**	**0.41**	**0.19**	**7.96**	**14.71**	**1.07**
	0.93	0.71	0.65	0.23	7.83	7.80	1.08
	0.93	0.60	0.58	0.10	8.97	22.26	1.10

	0.91	0.65	0.64	0.44	5.74	12.56	1.01
	0.95	0.76	0.54	0.35	9.01	13.93	1.02
	0.79	0.63	0.61	0.30	5.75	22.57	1.07
Svalbard	**0.95**	**0.76**	**0.54**	**0.35**	**9.01**	**13.93**	**1.02**
	0.94	0.74	0.69	0.50	8.13	19.39	1.40
Scandinavia	**0.95**	**0.76**	**0.54**	**0.35**	**9.01**	**13.93**	**1.02**
	0.93	0.71	0.65	0.23	7.83	7.80	1.08
	0.96	0.76	0.48	0.24	9.11	11.10	1.28
	0.95	0.72	0.41	0.19	7.96	14.71	1.07
North Asia	**0.94**	**0.74**	**0.69**	**0.50**	**8.13**	**19.39**	**1.40**
	0.95	0.76	0.54	0.35	9.01	13.93	1.02
	0.94	0.77	0.68	0.53	8.30	16.34	2.15
	0.96	0.74	0.67	0.30	9.17	24.59	1.68
	0.88	0.72	0.64	0.52	8.22	22.92	1.19
	0.99	0.74	0.64	0.24	7.38	21.88	1.46
Central Europe	**0.83**	**0.63**	**0.59**	**0.35**	**5.79**	**7.24**	**1.83**
	0.77	0.58	0.58	0.13	4.19	10.34	1.19
	0.86	0.69	0.68	0.32	4.35	8.51	1.02
	0.89	0.66	0.29	0.20	9.50	7.21	1.11
	0.90	0.58	0.53	0.25	8.85	7.90	3.64
	0.98	0.73	0.63	0.29	9.71	14.56	2.81
	0.87	0.62	0.61	0.21	9.75	7.67	2.19
	0.88	0.62	0.18	0.12	9.70	13.38	2.92
	0.98	0.69	0.60	0.35	9.76	23.50	2.62
Caucasus and Middle East	**0.90**	**0.71**	**0.53**	**0.28**	**8.29**	**5.03**	**3.32**
	0.85	0.63	0.59	0.41	9.79	5.72	2.98
	0.74	0.55	0.54	0.30	9.30	6.31	2.05
Central Asia	**0.94**	**0.74**	**0.69**	**0.50**	**8.13**	**19.39**	**1.40**
	0.94	0.77	0.68	0.53	8.30	16.34	2.15
	0.95	0.76	0.54	0.35	9.01	13.93	1.02
	0.96	0.74	0.67	0.30	9.17	24.59	1.68
	0.99	0.74	0.64	0.24	7.38	21.88	1.46
	0.88	0.72	0.64	0.52	8.22	22.92	1.19
South Asia West	**0.99**	**0.73**	**0.60**	**0.30**	**4.05**	**23.95**	**1.69**
	0.99	0.74	0.64	0.24	7.38	21.88	1.46
	0.94	0.77	0.68	0.53	8.30	16.34	2.15
	0.95	0.76	0.54	0.35	9.01	13.93	1.02
	0.96	0.74	0.67	0.30	9.17	24.59	1.68
	0.88	0.72	0.64	0.52	8.22	22.92	1.19
	0.94	0.78	0.60	0.23	5.88	19.24	1.75
	0.89	0.71	0.61	0.50	5.93	23.79	1.63
South Asia East	**0.91**	**0.73**	**0.67**	**0.56**	**5.32**	**8.57**	**1.55**
	0.94	0.77	0.68	0.53	8.30	16.34	2.15
	0.88	0.72	0.64	0.52	8.22	22.92	1.19

Low Latitudes	**0.94**	**0.74**	**0.69**	**0.50**	**8.13**	**19.39**	**1.40**
	0.96	0.74	0.67	0.30	9.17	24.59	1.68
	0.94	0.77	0.68	0.53	8.30	16.34	2.15
	0.88	0.72	0.64	0.52	8.22	22.92	1.19
	0.95	0.76	0.54	0.35	9.01	13.93	1.02
	0.99	0.74	0.64	0.24	7.38	21.88	1.46
Southern Andes	**0.95**	**0.76**	**0.54**	**0.35**	**9.01**	**13.93**	**1.02**
	0.88	0.72	0.64	0.52	8.22	22.92	1.19
	0.93	0.71	0.65	0.23	7.83	7.80	1.08
	0.94	0.74	0.69	0.50	8.13	19.39	1.40
	0.91	0.65	0.64	0.44	5.74	12.56	1.01
New Zealand	**0.94**	**0.74**	**0.69**	**0.50**	**8.13**	**19.39**	**1.40**
	0.88	0.72	0.64	0.52	8.22	22.92	1.19
	0.95	0.76	0.54	0.35	9.01	13.93	1.02
	0.99	0.74	0.64	0.24	7.38	21.88	1.46
	0.96	0.74	0.67	0.30	9.17	24.59	1.68

~~*Table S1 Equally plausible parameter sets for each RGI6 region.*~~

Table S2 Optimum regional parameter sets when we maximise the correlation coefficient between the simulated and observed specific mass balance.

Region	$\alpha_{vis,snow}$	$\alpha_{nir,snow}$	$\alpha_{vis,ice}$	$\alpha_{nir,ice}$	γ_{temp} (°K km^{-1})	γ_{precip} (%/100m)	γ_{wind}
Alaska	0.96	0.74	0.67	0.30	9.20	25.00	1.68
Western Canada and US	0.85	0.61	0.36	0.17	9.60	12.00	3.71
Arctic Canada North	0.99	0.74	0.64	0.24	7.40	22.00	1.46
Arctic Canada South	0.97	0.68	0.65	0.52	9.40	23.00	3.48
Greenland	0.99	0.71	0.32	0.15	9.20	20.00	2.12
Iceland	0.95	0.69	0.48	0.25	8.67	19.31	2.79
Svalbard	0.98	0.76	0.58	0.34	9.00	9.00	3.69
Scandinavia	0.96	0.74	0.67	0.30	9.20	25.00	1.68
Russian Arctic	0.95	0.69	0.48	0.25	8.67	19.31	2.79
North Asia	0.98	0.66	0.25	0.18	9.60	21.00	3.12
Central Europe	0.94	0.61	0.23	0.16	9.10	22.00	1.49
Caucasus and Middle East	0.98	0.66	0.25	0.18	9.60	21.00	3.12
Central Asia	0.98	0.66	0.25	0.18	9.60	21.00	3.12
South Asia West	0.97	0.75	0.44	0.12	7.70	17.00	3.77
South Asia East	0.86	0.61	0.57	0.28	8.70	22.00	3.95
Low Latitudes	0.97	0.68	0.65	0.52	9.40	23.00	3.48
Southern Andes	0.86	0.69	0.68	0.32	4.30	9.00	1.02
New Zealand	0.97	0.75	0.44	0.12	7.70	17.00	3.77
Mean	0.95	0.69	0.48	0.25	8.67	19.31	2.79

Table S3 Optimum regional parameter sets when we minimise the bias between the simulated and observed specific mass balance.

Region	$\alpha_{vis,snow}$	$\alpha_{nir,snow}$	$\alpha_{vis,ice}$	$\alpha_{nir,ice}$	γ_{temp} (°K km^{-1})	γ_{precip} (%/100m)	γ_{wind}
Alaska	0.88	0.63	0.42	0.24	8.20	19.00	1.21
Western Canada + US	0.87	0.72	0.56	0.33	6.00	10.00	2.25
Arctic Canada North	0.83	0.66	0.20	0.14	5.30	7.00	3.21
Arctic Canada South	0.82	0.66	0.16	0.12	9.30	21.00	1.74
Greenland	0.84	0.67	0.64	0.29	5.80	17.00	1.42
Iceland	0.90	0.71	0.52	0.27	7.53	17.38	1.84
Svalbard	0.95	0.76	0.54	0.35	9.00	14.00	1.02
Scandinavia	0.92	0.68	0.52	0.25	5.40	20.00	1.48
Russian Arctic	0.90	0.71	0.52	0.27	7.53	17.38	1.84
North Asia	0.94	0.74	0.69	0.50	8.10	19.00	1.40
Central Europe	0.76	0.51	0.48	0.19	4.90	24.00	3.73
Caucasus and Middle East	0.90	0.75	0.41	0.11	6.90	5.00	3.22
Central Asia	0.96	0.74	0.67	0.30	9.20	25.00	1.68
South Asia West	0.95	0.76	0.54	0.35	9.00	14.00	1.02
South Asia East	0.94	0.78	0.60	0.23	5.90	19.00	1.76
Low Latitudes	0.96	0.74	0.67	0.30	9.20	25.00	1.68
Southern Andes	0.95	0.76	0.54	0.35	9.00	14.00	1.02
New Zealand	0.96	0.74	0.67	0.30	9.20	25.00	1.68
Mean	0.90	0.71	0.52	0.27	7.53	17.38	1.84

Table S4 Comparison of percentage volume change relative to initial volume, from this study with Huss and Hock (2015)

Formatted: Caption, Keep with next

	This study ΔV % 2097-2011	Huss & Hock (2015) ΔV % 2100-2010	This study minus Huss & Hock (2015)
Alaska	-89±2	-58±14	-30
Western Canada and US	-100±0	-95±5	-5
Arctic Canada North	-47±3	-30±12	-9
Arctic Canada South	-74±8	-52±14	-22
Greenland	-31±5	-52±13	20
Iceland	-98±3	-62±18	-36
Svalbard	-68±16	-82±18	14
Scandinavia	-98±3	-96±4	-2
Russian Arctic	-79±10	-70±19	-7
North Asia	-71±5	-81±7	10
Central Europe	-99±0	-98±2	-1
Caucasus and Middle East	-100±0	-96±3	-4
Central Asia	-80±7	-88±7	8
South Asia West	-98±1	-87±9	-11
South Asia East	-95±2	-92±5	-3
Low Latitudes	-100±0	-98±0	-2
Southern Andes	-98±1	-44±14	-54

New Zealand	-88±5	-82±8	4

~~*Table S2 Comparison of percentage volume change relative to initial volume, from this study with Huss and Hock (2015)*~~

Formatted: Caption

Formatted: Caption, Keep with next

Formatted Table

	~~This study SLE mm 2097-2011~~	~~Huss & Hock (2015) SLE mm 2100-2010~~	~~Radic et al,.(2014) SLE mm 2100-2006~~	~~This study minus Huss & Hock (2015~~	~~This study minus Radic et al,.(2014)~~
~~Alaska~~	~~44.6±1.1~~	~~24.9±6.3~~	~~25.4~~	~~23.1~~	~~22.6~~
~~Western Canada and US~~	~~2.8±0.0~~	~~2.2±0.1~~	~~2.6~~	~~0.7~~	~~0.3~~
~~Arctic Canada North~~	~~35.8±3.0~~	~~19.7±7.8~~	~~42.2~~	~~15.1~~	~~-7.4~~
~~Arctic Canada South~~	~~18.1±2.1~~	~~9.9±2.8~~	~~15.0~~	~~10.1~~	~~5.0~~
~~Greenland~~	~~20.1±4.4~~	~~17.7±4.6~~	~~20.4~~	~~9.1~~	~~6.4~~
~~Iceland~~	~~9.3±0.3~~	~~4.7±1.7~~	~~4.9~~	~~5.4~~	~~5.2~~
~~Svalbard~~	~~17.0±4.6~~	~~13.9±3.1~~	~~15.8~~	~~5.0~~	~~3.1~~
~~Scandinavia~~	~~0.6±0.0~~	~~0.3±0.0~~	~~0.5~~	~~0.4~~	~~0.2~~
~~Russian Arctic~~	~~33.3±4.8~~	~~18.1±5.5~~	~~28.3~~	~~18.0~~	~~7.8~~
~~North Asia~~	~~0.3±0.0~~	~~0.2±0.0~~	~~0.6~~	~~0.1~~	~~-0.3~~
~~Central Europe~~	~~0.3±0.0~~	~~0.3±0.0~~	~~0.3~~	~~0.0~~	~~0.0~~
~~Caucasus and Middle East~~	~~0.2±0.0~~	~~0.1±0.0~~	~~0.2~~	~~0.1~~	~~0.0~~
~~Central Asia~~	~~8.0±0.7~~	~~9.2±1.1~~	~~11.9~~	~~-0.7~~	~~-3.4~~
~~South Asia West~~	~~8.1±0.1~~	~~6.2±1.0~~	~~7.1~~	~~2.5~~	~~1.6~~
~~South Asia East~~	~~1.9±0.0~~	~~2.4±0.7~~	~~3.5~~	~~-0.4~~	~~-1.4~~
~~Low Latitudes~~	~~0.2±0.0~~	~~0.2±0.0~~	~~0.5~~	~~0.0~~	~~-0.3~~
~~Southern Andes~~	~~14.4±0.1~~	~~5.8±1.8~~	~~8.5~~	~~9.7~~	~~7.0~~
~~New Zealand~~	~~0.1±0.0~~	~~0.1±0.0~~	~~0.1~~	~~0.0~~	~~0.0~~
~~Global~~	~~215.2±21.3~~	~~135.9±13.0~~	~~187.9~~	~~98.3~~	~~46.4~~

Table S5 Comparison of volume losses for this study with two other studies (Huss and Hock 2015, Radic et al. 2014). Volume loss is expressed in terms of sea level equivalent (mm). The last column lists volume losses when we correct the bias in the calibrated mass balance. There were no observations available to calibrate the present-day mass balance for Iceland and the Russian Arctic, so there is no bias corrected volume loss for these regions.

Formatted: Caption, Keep with next

Formatted Table

Formatted: Left

	This study 2097-2011	Huss 2100-2010	Radic 2100-2006	This study minus Hock	This study minus Radic	Bias corrected
Alaska	44.6±1.1	24.9±6.3	25.4	23.1	22.6	45.0±1.1
Western Canada and US	2.8±0.0	2.2±0.1	2.6	0.7	0.3	2.2±0.0
Arctic Canada North	35.8±3.0	19.7±7.8	42.2	15.1	-7.4	37.8±2.9
Arctic Canada South	18.1±2.1	9.9±2.8	15.0	10.1	5.0	18.3±2.2
Greenland	20.1±4.4	17.7±4.6	20.4	9.1	6.4	21.9±4.3
Iceland	9.3±0.3	4.7±1.7	4.9	5.4	5.2	-

Svalbard	17.0±4.6	13.9±3.1	15.8	5.0	3.1	15.6±4.6
Scandinavia	0.6±0.0	0.3±0.0	0.5	0.4	0.2	0.8±0.0
Russian Arctic	33.3±4.8	18.1±5.5	28.3	18.0	7.8	-
North Asia	0.3±0.0	0.2±0.0	0.6	0.1	-0.3	0.2±0.0
Central Europe	0.3±0.0	0.3±0.0	0.3	0.0	0.0	0.4±0.0
Caucasus and Middle East	0.2±0.0	0.1±0.0	0.2	0.1	0.0	0.2±0.0
Central Asia	8.0±0.7	9.2±1.1	11.9	-0.7	-3.4	6.0±0.8
South Asia West	8.1±0.1	6.2±1.0	7.1	2.5	1.6	7.9±0.1
South Asia East	1.9±0.0	2.4±0.7	3.5	-0.4	-1.4	1.7±0.0
Low Latitudes	0.2±0.0	0.2±0.0	0.5	0.0	-0.3	0.2±0.0
Southern Andes	14.4±0.1	5.8±1.8	8.5	9.7	7.0	7.6±0.3
New Zealand	0.1±0.0	0.1±0.0	0.1	0.0	0.0	0.01±0.0
Global	215.2±21.3	135.9±13.0	187.9	98.3	46.4	222.5±20.1

~~*Table S3 Comparison of volume losses for this study with (Huss and Hock 2015, Radic et al. 2014). Volume loss is expressed in terms of sea level* equivalent (mm)~~

Table S6 Comparison of modelled and observed energy balance components at five elevation levels on the Pasterze glacier, Austria. Information about the observations are detailed in Greuell and Smeets (2001). The table contains data from two experiments, the first where wind speed in not tuned (γ_{wind} = 1) and the second where wind speed is increased to four times the surface wind speed (γ_{wind} = 4).

Elevation		Observations	γ_{wind} = 1	γ_{wind} = 4
2205m	Incoming short-wave radiation (Wm^{-2})	256.0	262.9	262.9
	Albedo (visible)	0.2	0.1	0.2
	Incoming long-wave radiation (Wm^{-2})	299.0	295.7	295.7
	Outgoing long-wave radiation (Wm^{-2})	315.0	305.8	309.5
	Elevated air temperature (°C)	6.8	9.1	9.1
	Surface temperature (°C)	-0.1	-1.5	-0.7
	Roughness length (mm)	2.6	3.0	3.0
	Sensible heat flux (Wm^{-2})	**48.0**	**0.2**	**22.2**
	Latent heat flux (Wm^{-2})	10.0	0.2	13.0
	Net radiation on tiles (Wm^{-2})	282.2	223.7	219.1
	Wind speed (ms^{-1})	**4.1**	**1.1**	**4.3**
	Ablation rate (mm water equivalent day^{-1})	61.3	52.7	58.4
2310m	Incoming short-wave radiation (Wm^{-2})	272.0	262.9	262.9
	Albedo (visible)	0.3	0.1	0.2
	Incoming long-wave radiation (Wm^{-2})	299.0	295.7	295.7
	Outgoing long-wave radiation (Wm^{-2})	315.0	305.8	309.6
	Elevated air temperature (°C)	6.4	8.4	8.4
	Surface temperature (°C)	-0.1	-1.5	-0.6
	Roughness length (mm)	1.2	3.0	3.0
	Sensible heat flux (Wm^{-2})	**53.0**	**0.2**	**21.5**
	Latent heat flux (Wm^{-2})	11.0	0.2	12.7
	Net radiation on tiles (Wm^{-2})	283.1	223.4	218.5
	Wind speed (ms^{-1})	**4.5**	**1.1**	**4.3**
	Ablation rate (mm water equivalent day^{-1})	63.1	52.6	57.9
2420m	Incoming short-wave radiation (Wm^{-2})	278.0	262.9	262.9
	Albedo (visible)	0.3	0.2	0.2
	Incoming long-wave radiation (Wm^{-2})	296.0	295.7	295.7

Formatted: Font:

Field Code Changed

Formatted: Caption

Field Code Changed

Formatted: Font: Not Italic

Formatted Table

Formatted: Font: Not Bold

Formatted: Font: Not Bold

	Outgoing long-wave radiation (Wm^{-2})	315.0	305.8	309.7
	Elevated air temperature (°C)	7.1	7.6	7.6
	Surface temperature (°C)	-0.1	-1.5	-0.6
	Roughness length (mm)	5.8	3.0	3.0
	Sensible heat flux (Wm^{-2})	**63.0**	**0.1**	**20.7**
	Latent heat flux (Wm^{-2})	10.0	0.1	12.1
	Net radiation on tiles (Wm^{-2})	315.5	218.2	212.7
	Wind speed (ms^{-1})	**4.6**	**1.1**	**4.3**
	Ablation rate (mm water equivalent day^{-1})	66.9	51.3	56.3
2945m	Incoming short-wave radiation (Wm^{-2})	307.0	262.9	262.9
	Albedo (visible)	0.6	0.4	0.4
	Incoming long-wave radiation (Wm^{-2})	282.0	295.7	295.7
	Outgoing long-wave radiation (Wm^{-2})	314.0	307.7	311.0
	Elevated air temperature (°C)	3.5	4.2	4.2
	Surface temperature (°C)	-0.3	-1.1	-0.3
	Roughness length (mm)	1.3	3.0	3.0
	Sensible heat flux (Wm^{-2})	**23.0**	**1.3**	**15.9**
	Latent heat flux (Wm^{-2})	5.0	1.2	9.1
	Net radiation on tiles (Wm^{-2})	139.9	183.4	178.3
	Wind speed (ms^{-1})	**4.3**	**1.1**	**4.3**
	Ablation rate (mm water equivalent day^{-1})	32.1	46.0	50.7
3225m	Incoming short-wave radiation (Wm^{-2})	286.0	262.9	262.9
	Albedo (visible)	0.6	0.5	0.5
	Incoming long-wave radiation (Wm^{-2})	274.0	295.7	295.7
	Outgoing long-wave radiation (Wm^{-2})	313.0	308.0	310.7
	Elevated air temperature (°C)	3.2	2.6	2.6
	Surface temperature (°C)	-0.7	-1.0	-0.4
	Roughness length (mm)	2.0	3.0	3.0
	Sensible heat flux (Wm^{-2})	**20.0**	**2.4**	**11.5**
	Latent heat flux (Wm^{-2})	1.0	2.2	6.9
	Net radiation on tiles (Wm^{-2})	115.4	169.8	165.4
	Wind speed (ms^{-1})	**4.4**	**1.1**	**4.3**
	Ablation rate (mm water equivalent day^{-1})	24.0	43.5	47.3

Greuell, W. & P. Smeets (2001) Variations with elevation in the surface energy balance on the Pasterze (Austria). *Journal of Geophysical Research-Atmospheres,* 106**,** 31717-31727.

Huss, M. & R. Hock (2015) A new model for global glacier change and sea-level rise. *Frontiers in Earth Science,* 3.

Radic, V., A. Bliss, A. C. Beedlow, R. Hock, E. Miles & J. G. Cogley (2014) Regional and global projections of twenty-first century glacier mass changes in response to climate scenarios from global climate models. *Climate Dynamics,* 42**,** 37-58.

Formatted: Font: Not Bold

Formatted: Font: Not Bold

Formatted: Font: Not Bold

Formatted: Indent: Left: 0 cm, First line: 0 cm